Comparative gene expression in different stages of *Mycobacterium tuberculosis* infection in mice

Soomin Park

Department of Medical Science

The Graduate School, Yonsei University

Comparative gene expression in different stages of *Mycobacterium tuberculosis* infection in mice

Directed by Professor In-Hong Choi

The Master's Thesis

submitted to the Department of Medical Science,

the Graduate School of Yonsei University

in partial fulfillment of the requirements for the degree of

Master of Medical Science

Soomin Park

December 2016

연세대학교
YONSEI UNIVERSITY

This certifies that the Master's Thesis

of Soomin Park is approved.

_____

Thesis Supervisor : In-Hong Choi

_____

Thesis Committee Member#1 : Sang-Nae Cho

_____

Thesis Committee Member#2 : Kyungwon Lee

The Graduate School

Yonsei University

December 2016

ACKNOWLEDGEMENTS

석사과정 동안 아낌없이 도움주신 최인홍 교수님께 진심으로 감사드립니다. 교수님께서는 저에게 학문적으로, 인격적으로 너무나 큰 본보기가 되어 주셨고, 그 덕분에 흔들림 없이 학위과정을 잘 마칠 수 있었습니다. 교수님의 제자로 공부하고 실험하고 토론하는 모든 순간이 행복했습니다.

심사위원 조상래 교수님과 이경원 교수님께도 감사의 마음을 전합니다. 결핵과 진단의 대가 교수님들께 조언을 받을 수 있어서 영광이었습니다. 특히 조상래 교수님께서 제공해 주신 샘플 덕분에 학위논문을 완성할 수 있었으며, 조금이라도 더 질 좋은 논문이 될 수 있도록 도움 주셔서 감사드립니다.

또한 같은 길을 가는 동료이자 스승이었던 학위과정 내내 함께한 실험실 식구들 서진원 선생님, 장지영 선생님, 한구 그리고 장영생 박사님께 감사드립니다. 실험실 안팎에서 일어난 크고 작은 일을 나누던 인생의 멘토 이강무 박사님, 양창모 선생님, 그리고 너무 소중한 친구 수정, 혜진, 희로애락을 함께 한 정민, 유진, 화영에게도 감사드립니다.

마지막으로 존경하고 사랑하는 아버지 박원욱, 어머니 김유진, 오빠 박철우 그리고 하나님께 깊이 감사드립니다. 혼자 힘으로는 해내지 못 했을 거라는 걸 잘 압니다. 존재만으로도 충분히 힘이 되고 든든하며 행복합니다. 이제는 제가 그 은혜에 보답해 나가겠습니다. 사랑합니다.

박수민 드림

TABLE OF CONTENTS

LIST OF FIGURES

LIST OF TABLES

ABBREVIATION

TB	**tuberculosis**
***M. tb* (MTB)**	***Mycobacterium tuberculosis***
RT-qPCR	**real-time reverse transcription quantitative polymerase chain reaction**
CCL	**chemokine (C-C motif) ligand**
CXCL	**chemokine (C-X-C motif) ligand**
MCP	**monocyte chemoattractant protein**
IL	**interleukin**
IFN-γ	**interferon-γ**
TNF	**tumor necrosis factor**
MiRNA	**microRNA**
pri-miRNA	**primary miRNA**
pre-miRNA	**precursor miRNA**

Abstract

Comparative gene expression in different stages of *Mycobacterium tuberculosis* infection in mice

Soomin Park

Department of Medical Science

The Graduate School, Yonsei University

(Supervised by Professor In-Hong Choi)

Tuberculosis (TB) is an infectious disease caused by *Mycobacterium tuberculosis*. One-third of the world's population is estimated to be latently infected with *M. tuberculosis*; however, only approximately 10% of latently infected people will develop this overt disease, and their aerosol droplets can be transmitted through the air. Current tests available for the diagnosis of TB are limited by their inability to differentiate between latent tuberculosis infection (LTBI) and active TB disease. Therefore, an accurate and effective marker for differential diagnosis should be developed for predicting disease progression.

Given the increasing interest in identifying new biomarkers against TB, we examined promising biomarkers that could distinguish between chronic/reactivation TB disease and LTBI using an *M. tuberculosis*-infected mouse model. The lung tissue and serum of C57BL/6 mice were used to identify the differences of gene expression among healthy, LTBI, chronic

TB, spontaneous reactivation, and immunosuppressive drug-treated groups.

First, microarray analysis using isolated mRNAs from mice tissues showed several important immune-related genes with different expression levels between the chronic/latent and healthy control groups ($p < 0.05$). Next, quantitative reverse transcription-polymerase chain reaction to validate the results obtained by the microarray was performed. Based on the cDNA microarray results, 17 candidate genes were selected and clustered into four groups: 1) chemokines excluding monocyte chemoattractant proteins (MCPs) (CXCL9, CXCL10, CXCL11, CCL5, CCL19); 2) MCPs (CCL2, CCL7, CCL8, CCL12); 3) Receptors (IL2Rβ, IL7R, IL12Rβ1, IL12Rβ2, IL21R, IL27Rα); and 4) TNF and IFN-γ genes. Results from the cDNA microarray and quantitative RT-PCR analyses revealed that expression of the selected cytokine genes was significantly higher in lung tissues of the chronic stage than of the latent stage. CXCL9, CCL7, CCL12 were noticeably increased in the chronic stage compared with those in the latent stage. Therefore, these three significantly increased cytokines in lung tissue from the mouse TB model might be candidates for biomarkers that distinguish the two disease stages. This information can be combined with already reported potential biomarkers to construct a network of more efficient TB markers. We used Luminex assays to confirm the same tendency of gene expression in mice serum.

Second, there is a substantial need for biomarkers to distinguish latent, chronic TB from spontaneous reactivation, for predicting disease progression. To identify the immunological status of the latent, chronic, and reactivation stages, immunological genes were analysed in lung tissues from mice infected with *M. tuberculosis*. Gene expression was screened using cDNA microarray analysis and confirmed by quantitative RT-PCR using isolated microRNAs from mice tissues. In the result, 10 microRNAs (mmu-miR-1a-3p, mmu-miR-133a-5p, mmu-miR-133a-3p, mmu-miR-206-3p, mmu-miR-133b-3p, mmu-miR-3064-5p, mmu-miR-450b-3p, mmu-miR-26b-3p, mmu-miR-181a-2-3p, mmu-miR-8114) were likely to be the biomarkers that can distinguish between latent and reactivation TB. Specifically, mmu-miR-

206-3p was noticeably increased in the reactivation stage compared with the latent and chronic stage. And mmu-miR-1a-3p is expected to be a biomarker candidate that can simultaneously distinguish latent, chronic, and reactivation stages.

In conclusion, these findings suggest that the protective mechanisms against TB infection may be related to chemokines, MCPs, chemokine receptors and microRNAs that modulate the activity of immune responses, and some of which are potential biomarkers distinguishing different stages of *M. tuberculosis* infection.

Key Words: Tuberculosis, Cytokine, Chemokine, MicroRNA, Latent, Chronic, Reactivation, Bupropion, Dexamethasone

I. Introduction

Tuberculosis (TB) is still prevalent worldwide and is regarded as one of the most serious infectious diseases.[1] According to the 2015 announcement of the World Health Organization, 9.6 million people were newly affected with TB, and there were 1.5 million deaths due to TB in 2014. The main cause of TB is *Mycobacterium tuberculosis* (Mtb). One-third of the world's population has a latent TB infection (LTBI) by *M. tb*,[2] and they are asymptomatic. Although only 5–10% of LTBI cases can develop into active TB, a higher risk of reactivation is associated with drug resistance of the bacteria or immunosuppression.[3] By contrast, active TB patients are infectious and symptomatic.

Bacillus Calmette-Guerin (BCG) is currently the only TB vaccine, but it has been reported that it will be less effective at over 10 years after vaccination.[4] The tuberculin skin test (TST) and interferon-gamma release assay (IGRA) are commonly used to diagnose TB infection. The TST is a method of injecting a purified protein derivative of *M. tuberculosis* in the skin; BCG and several non-tuberculous mycobacteria show cross-reactivity because they share common major antigens.[5] It takes 48–72 hr to obtain a diagnostic result with this test, and it is affordable. The IGRA is a method of stimulating lymphocytes with the TB-specific antigens such as early secretory antigen target 6 (ESAT6) or culture filtrate protein 10 (CFP10) followed by measuring the concentration of IFN-γ secreted *ex vivo* or by counting the cells capable of secreting IFN-γ. The IGRA does not have cross-reactivity to BCG but still shows reactivity against several types of non-tuberculous mycobacteria. Although it is more expensive than TST, it only takes 24 hr to obtain a diagnosis result, and it is a more sensitive.[6] However, both of these diagnostic tests have low specificity and often give false positive results. Furthermore, both tests have a critical limitation in that they cannot distinguish between LTBI and active TB.[7] Thus, development of a TB diagnostic method that is more sensitive, efficient, and specific is urgently needed.

Besides being able to distinguish between only healthy and active TB, recent research has focused on identifying a marker that can distinguish between LTBI and active TB.[8] An ideal biomarker is one that can be easily obtained from patients, and most importantly, should be a specific gene related to a key biological process that is expressed differently depending on whether the individual's status is healthy, LTBI, or active TB. One method to find more suitable biomarkers of TB is to compare the cytokines in sera from patients with active or latent stages of infection with those from healthy individuals.[9-11] However, consistent results have not been obtained because the number of cytokines analysed is often too small, and the types of assays used to detect them vary between studies. Thus, a more systematic approach for analysing all cytokines is needed, and the results obtained can be combined with reported TB biomarkers to construct a network of potential markers. This study therefore aimed to identify cytokines that could be superior to or used in combination with IFN-γ for the rapid diagnosis of TB and for distinguishing between latent and active infections.

Instead of human samples, lung tissues from mice infected with *M. tb* strain Erdman, which was established by our group were analysed. Because of their heterogeneous genetic background, human samples such as peripheral blood lymphocytes or plasma often show diverse immune responses, and, moreover, may reflect an indirect phenomenon far from the pathological lesions. Therefore, it was suggested that an animal study would deliver consistent information of *in situ* immune responses because infected lung tissues from the same genetic background were being evaluated. Through cDNA microarray and quantitative RT-PCR analyses, information on immune response-related genes expressed differentially according to the latent and chronic stages was obtained, and biomarker candidates to distinguish the two infection stages of TB were identified.

The regulation of gene expression by miRNAs is also affected by *M. tb* infection. Although the expression of the immune-related gene by tuberculosis infection is accompanied by

complex boosting, miRNAs bind specifically to target mRNA so they might be able to elucidate more specific immune mechanisms than cytokines and chemokines. Using miRNAs as a means of diagnosis is also expected to result in more specific and sensitive results.

MicroRNA (miRNA) consists of 21–25 nucleotides, and is a highly conserved and single-stranded noncoding RNA that can regulate the gene expression level through post-transcriptional regulation.[12] miRNA transcription occurs in the nucleus by RNA polymerase II or III; it is made of a hairpin-shaped primary miRNA (pri-miRNA) comprised of approximately 70 nucleotides. A pri-miRNA that is cleaved by the RNase III enzyme drosha is transported to the cytoplasm by exportin 5, which is referred to as double-stranded precursor miRNA (pre-miRNA). The end of the hairpin of pre-miRNA is cleaved by dicer, and processed to mature miRNA of approximately 22 nucleotides. One of the two strands binds to the RISC complex and then it binds to the 3′ untranslated regions of intracellular target mRNAs. Given that miRNA binding to the target mRNAs controls the immune response, inducing mRNA degradation or suppressing translation,[13] it plays an important role in biological processes such as cell differentiation, proliferation, and development.[14]

miRNA is regarded as an attractive biomarker because it is very stable under freezing, thawing, heat, acidic, and alkaline conditions,[15] and therefore has potential for therapeutic use in targeting mRNA using a mimic or inhibitor. Although several diagnostic biomarkers have been identified for various types of cancer to date, the role of miRNAs in the susceptibility and resistance to infectious diseases such as TB remains largely unknown.[16]

In this study, we established a mouse model of *M. tuberculosis* infection. Total RNA was isolated from the lung tissue of the mice at each stage of infection. The primary aim of the study was to find a potential biomarker that can distinguish between the TB infection stages by analyzing the difference in the expression of cytokine/chemokine-related genes and in quantity of miRNA.

II. Materials and methods

1. Animal model

A. Bacterial strains

M. tuberculosis strain, Erdman (Colorado State University, Fort Collins, CO) was grown in Middlebrook 7H9 broth (Difco, Oxford, UK) supplemented with 0.05% Tween 80 and ADC enrichment. All the experimental protocols included in this study were approved by the Institutional Animal Care and Use Committees (IACUCs) (2014-0301).

B. Mouse infection, therapy, and activation

C57BL/6 mice were infected through the aerosol route with *M. tuberculosis* at 200–300 colony forming units (CFUs)/lung using a Glas-col aerosol exposure system. They were treated with TB drugs beginning at 4 wk post-infection. As the first therapy, the infected mice were treated with isoniazid (INH) and pyrazinamide (PZA) for 5 wk, and then subsequently treated with INH and ethambutol (EMB) for another 3 wk. The drugs were delivered *ad libitum* by adding the following concentrations to drinking water: 100 μg/ml INH, 600 μg/ml EMB, and 600 μg/ml PZA. All of the drug-containing water was replaced weekly. Water consumption was monitored to determine the delivered daily dose (INH: 26.5 ± 0.9 mg/kg, PZA and EMB: 132.6 ± 4.7 mg/kg). To maintain the latent state of TB infection, the mice that completed the drug therapy were supplied with regular drinking water for one week.

To establish reactivation, two immune-suppressing agents were provided to the latent TB mice. Two hundred microliters of bupropion hydrochloride (11.5 mg/ml in phosphate buffered saline [PBS], Tokyo Chemical Industry Co.) or dexamethasone sodium phosphate (2.63 mg/ml in PBS, Matrix Scientific) was intraperitoneally injected into each latent mouse twice

per week for 4-6 wk. Over the period of reactivation, to enhance the metabolic activity of the mice, drinking water containing 1 ml/l hexanoic acid (Sigma, Poole, UK) was provided for 5 wk.

Chronic TB mice were sacrificed at 16 wk post-infection without receiving any TB drug or immune-suppressant treatment. Four to five mice were sacrificed from each group, the lungs and spleens were homogenized in PBS, and the dilutions were plated on 7H10 agar to enumerate the CFUs.

C. Histopathology

One lung was fixed in 4% phosphate-buffered formaldehyde and embedded in paraffin. Approximately 5-μm-thick sections were prepared and stained with hematoxylin and eosin (H&E). Acid-fast *M. tuberculosis* bacilli in the lung tissue were detected by Ziehl-Neelsen staining. The stained slides were observed under a light microscope.

2. Cytokine detection

A. RNA isolation

Total RNA was isolated using RNeasy Mini Kit (Qiagen, Valencia, CA) from the lung tissues of healthy, latent, and chronic TB mice. The quality and quantity of total RNA was assessed by measuring the ratio of absorbance of total RNA at 260/280 nm and 260/230 nm with the NanoDrop-2000 spectrophotometer (Thermo Fisher Scientific, Wilmington, DE, USA), and the 28S/18S ratio and RNA integrity number (RIN) were determined with Bioanalyzer.

B. Microarray

A GeneChip® (Mouse Gene 2.0 ST Array X 21; Affymetrix, Santa Clara, CA) containing more than 698,000 total probes and 26,515 RefSeq (Entrez) genes was used in this study. Samples were prepared and handled according to the manufacturer's recommendation. Genes with a significant difference in transcription level were selected for further analysis when the expression values changed by 2-fold or greater and when $p < 0.05$ was obtained in the student *t*-test.

C. cDNA synthesis

For cDNA synthesis, reverse transcription (RT) reactions were performed with M-MLV Reverse Transcriptase (Invitrogen, Carlsbad, CA, USA). Each 40-μl RT reaction mix included 8 μl of 5X FS buffer, 8 μl of dNTPs (2.5 mM), 1 μl of oligo dT (0.5 μg/μl), 2 μl of M-MLV RT, 4 μl of dithiothreitol (0.1 M), 3 μg of RNA template, and RNase-free water for each sample. This mixture was incubated at 42°C for 2 hr.

D. Real-time RT-qPCR validation

All of the DNA oligonucleotides and the housekeeping gene glyceraldehyde-3-phosphate dehydrogenase (*Gapdh*) primers were synthesized using the IDT real-time PCR primer design program. Real-time PCR was performed with Power FastStart Universal SYBR Green Master (Rox) (Roche Diagnostics, Indianapolis, IN, USA) using the 7500 Real-Time PCR system (Applied Biosystems, Foster City, CA, USA). One microliter of cDNA was added to a PCR mixture that consisted of 12.5 μl of FastStart SYBR green master mix, 11 μl of RNase-free water, and 10 μM of each primer. The real-time PCR running protocol was 10 min at 95°C,

followed by 40 cycles of 95°C for 15 sec and 60°C for 1 min. The dissociation curve was obtained by heating from 60°C to 95°C.

For data analysis, the Step One software v2.0.2 (Applied Biosystems) was used to calculate the levels of target gene expression in samples relative to the level of expression in the control samples with the comparative cycle threshold method (ΔΔCT). Expression values for target genes were normalized to the expression of *gapdh*.

E. Luminex assay

Magnetic Luminex Screening Assay (R&D Systems, Minneapolis, MN, USA) is specially designed to optimize the benefits and overcome the challenges of multiplexing. CCL7 and CCL12 were measured using mice chemokine panels. Samples were performed at 1:2 dilution in assay diluent in order to optimize the expected CCL7, CCL12 concentrations in the antigen tube to the range of the standard curve. We utilized xMAP microparticle technology (Luminex Corporation, Austin, TX, USA) and data were collected using the xPONENT software version 3.0.380.0. (Luminex). Assays were performed according to the manufacturers' instructions. Concentrations of cytokines (pg/ml) were determined on the basis of the fit of a standard curve for mean fluorescence intensity versus pg/ml. (n=3 mice per group)

3. MiRNA detection

A. RNA isolation

Total RNA was isolated using miRNeasy Mini Kit (Qiagen, Valencia, CA) from the lung tissues of the healthy, latent, chronic TB, spontaneous reactivation, bupropion and dexamethasone-treated mouse models. The quality and quantity of total RNA was assessed

by measuring the ratio of absorbance of total RNA at 260/280 nm and 260/230 nm with the NanoDrop-2000 spectrophotometer (Thermo Fisher Scientific, Wilmington, DE, USA) and Qubit (Thermo Fisher Scientific, Wilmington, DE, USA); 28S/18S and the RIN were determined with Bioanalyzer.

B. Microarray

A GeneChip® (Mouse miRNA 4.0 Array X 12; Affymetrix, Santa Clara, CA) containing 30,434 total mature miRNA probe sets and 1,908 mouse mature miRNA probe sets was used in this study. Samples were prepared and handled according to the manufacturer's recommendations. Significantly expressed transcripts were selected when expression values changed by 1.5-fold or greater and $p < 0.05$ was obtained from the t-test. The Affymetrix Expression console 1.3.1, R program (3.0.2), TargetScan 6.2, and DAVID 6.7 software were used for analyses.

C. Reverse transcription

For cDNA synthesis, RT reactions were performed with a Taqman MicroRNA Reverse Transcription kit (Applied Biosystems, Foster City, CA, USA). Each 15-μl RT reaction mix consisted of 0.15 μl of 100 mM dNTPs (with dTTP), 1 μl of MultiScribe Reverse Transcriptase (50 U/μl), 1.5 μl of 10X Reverse Transcription Buffer, 0.19 μl of RNase inhibitor (20 U/μl), 4.16 μl of nuclease-free water, 3 μl of 5X primer, and 5 μl of the RNA sample. This mixture was incubated on ice for 5 min. RT was performed using 1 cycle of 16°C for 30 min, 42°C for 30 min, 85°C for 5 min, and held at 4°C.

D. Real-time RT-qPCR validation

U6 snRNA was used for RT-PCR with the TaqMan™ microRNA Control Assay (Thermo Fisher Scientific, Wilmington, DE, USA). The real-time PCR mixture included 1 μl of TaqMan MicroRNA Assay product (20X), 1.33 μl of the product from the RT reaction, 10 μl of TaqMan 2X Universal PCR Master Mix, No AmpErase UNG (Thermo Fisher Scientific, Wilmington, DE, USA), and 7.67 μl of nuclease-free water. Real-time PCR was performed with 1 cycle of 95°C for 10 min, and 40 cycles of 95°C for 15 sec and 60°C for 60 sec. Real-time PCR was performed with the 7500 Real-Time PCR system (Applied Biosystems, Foster City, CA, USA).

For data analysis, the Step One software v2.0.2 (Applied Biosystems) was used to calculate the levels of target gene expression in samples relative to the level of expression in the control samples with the comparative cycle threshold method (ΔΔCT). Expression levels for target genes were normalized to the expression of *Gapdh*.

E. Statistical analysis

Results are presented as the mean and standard error of the mean (SEM). For CFU and RT-qPCR analysis, the nonlinear regression (curve fit) and the Student's unpaired *t*-test (two-tailed) was used, respectively. Data were analyzed using the Graph Pad Prism version 5.01 program (GraphPad Software Inc., USA). A p-value < 0.05 was considered statistically significant.

III. Results

1. Animal model

A. A new mouse model of Mtb infection based on histopathological analysis.

A mouse model for Mtb infection was developed and used for this study, based on our previous Cornell mouse models mimicking human infection in terms of infection route, treatment, and relapse which were confirmed by colony-forming unit (CFU) counts (Fig.1a). For immunological and biological analysis of each stage of infection, we modified the traditional Cornell model.

First, latent state of disease was determined based on pathological recovery, i.e. disappearance of lung lesions following two steps of drug therapy, even though Mtb bacteria were detected in some mouse lungs after the therapy. Previous our Cornell model indicated “no” Mtb colony on agar plate as latent state of disease, but this state contained two mouse populations, actual latent disease mouse with relapse potential and completely treated healthy mouse, which is a valid model when used for vaccine studies. Because reactivated mice can be counted to determine the effectiveness of the vaccine. However, it is not suitable as a model for our experiments to identify immune activities or use them to find biomarkers. Counting the number of colonies in an agar medium is only a part of how viability is measured. Instead, in current model of a combination of drugs with low killing effect, we made below 100 CFU that they are known to be statistically insignificant and they were named as "latency" (pathology-based not CFU-based). This latent state includes merely mice with latent disease amenable to relapse in the future, thereby all treated mice were spontaneously relapsed. We have constructed a new animal model and it is of great significance that we have used only the homogenous latent disease mouse population except for the healthy one.

Second, we excluded immunosuppressant for reactivation, because a specific

immunosuppressant use causes artificial change of immune response and impedes our effort to reveal immunological change during relapse by other factors such as host's senescence, other co-infections, environmental and health changes. This model allows us to identify reliable changes in the immune response.

Third, the period of producing latent and chronic states is much shorter than the existing models. The old model was 18 weeks to latent and 54 weeks to reactivation, but this model used takes 14 weeks to complete latent and 18 weeks to reactivation. Shortening the period of infection can be considered to accelerate the development of vaccines, therapeutic agents, pathology research, and diagnostic biomarkers.

To induce a chronic infection in mice that is comparable to an active infection in humans, one group of mice was not treated with any anti-TB agents for 16 weeks after aerosol infection initiating with 200–300 CFU of Mtb. To mimic latent infection, another group of mice was administered with isoniazid (INH) and pyrazinamide (PZA) from the 4^{th} to 9^{th} weeks of postinfection, which was followed by INH and ethambutol (EMB) from the9^{th} to 12^{th} weeks. The latent stage was pathologically confirmed and there was no significant reactivation of bacilli growth without further administration of anti-TB agents from the 12^{th} to 14^{th} weeks of postinfection. Upon reactivation, the CFU increased by more than 10^4 in the lungs and 10^3 in the spleens at the 18^{th} week of postinfection (Figure 1A).

For the chronic stage in untreated mice, the CFU reached to more than 10^5 in the lungs and more than 10^4 in the spleens at 16 weeks after aerosol infection. For induction of the latent stage, the CFU declined to less than 10^2 in both lungs (Figure 1B) and 10^1 in the spleens (Figure 1C) at 9 weeks after INH+PZA and INH+EMB treatment. We denoted latent stage-1 and latent stage-2 as one day and one week after completion of drug treatment.

(A)

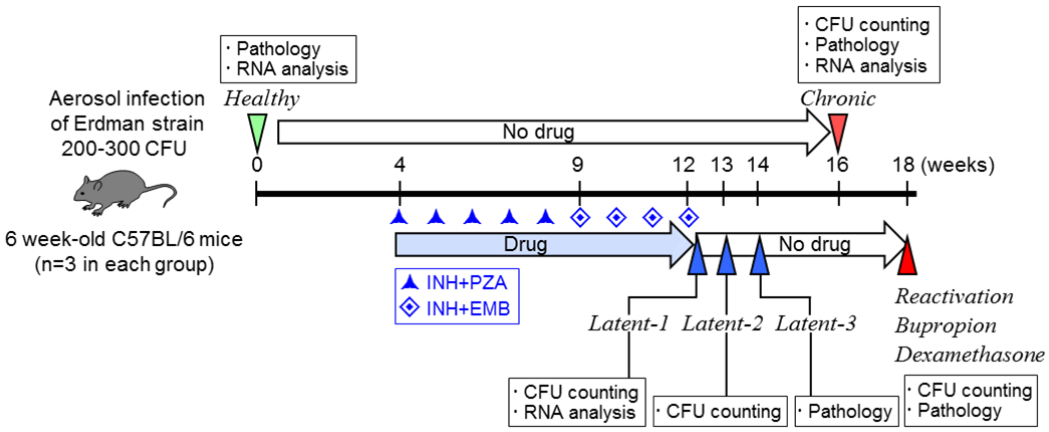

(B)

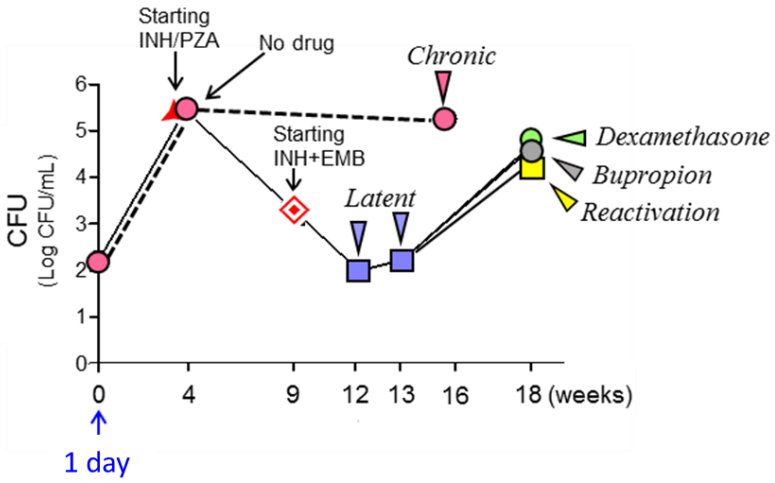

(C)

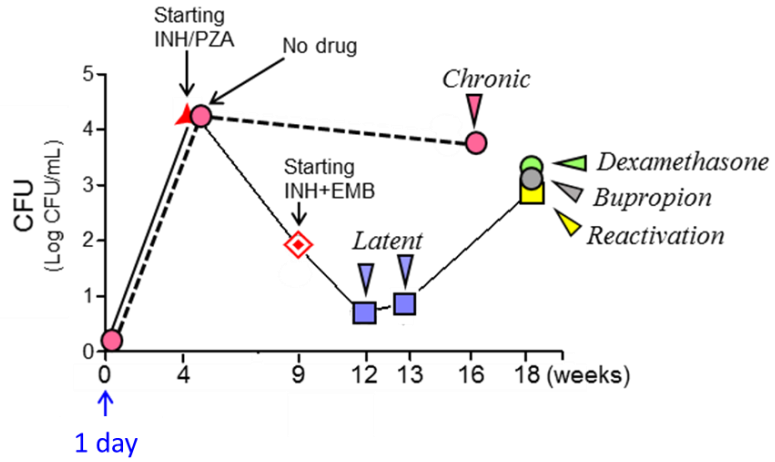

Figure 1. Animal infection and drug treatment. Schematic representation of the animal model (A), and bacterial burden in the lungs (B) and spleens (C) of C57BL/6 mice infected with *M. tuberculosis*.

B. Histological examination of the lung tissue

To confirm the difference in the infection status depending on the CFUs of *M. tuberculosis*, granulomatous inflammation was observed with a microscope by fixing and H&E staining a lobe of the lung at each stage of infection. Histopathology of lung tissues of chronic stage revealed multiple dispersed granulomas-like structure, infiltrated mostly with macrophages and neutrophils (Figure 2C) compared to those in the lungs of healthy mice (Figure 2A). At latent stage-1, some pathology of active infection was still observed (data not shown), suggesting the tissues had not fully recovered from the inflammation. The granuloma formation and inflammation were meaningfully reduced at latent stage-3, which was 2 weeks after the completion of drug treatment (Figure 2B), suggesting a stable latent stage had been reached. These results verified that current mouse model established in this study is quite comparable to each stage of Mtb infection in humans. This latent infection turned to active infection indicated by multiple granuloma-like formation of reactivation stage (Figure 2D), which was observed at 6 weeks after no anti-TB drug treatment following completion of the INH+PZA and INH+EMB treatment. Mice that were then fed only water at the same level as immunosuppressive drugs such as bupropion (Figure 2E) and dexamethasone (Figure 2F) showed a subsequent increase in granulomatous inflammation. The spontaneous reactivation mice and the immunosuppressant treated mice were confirmed to have similar pathological conditions by CFU and histological examination. This indicated that spontaneous reactivation could take place without immunosuppressive drug treatment, confirming that a model for the reactivation of TB excluding the influence of the drug was successfully established. Therefore, the effect of drugs on spontaneous reactivation can be ruled out.

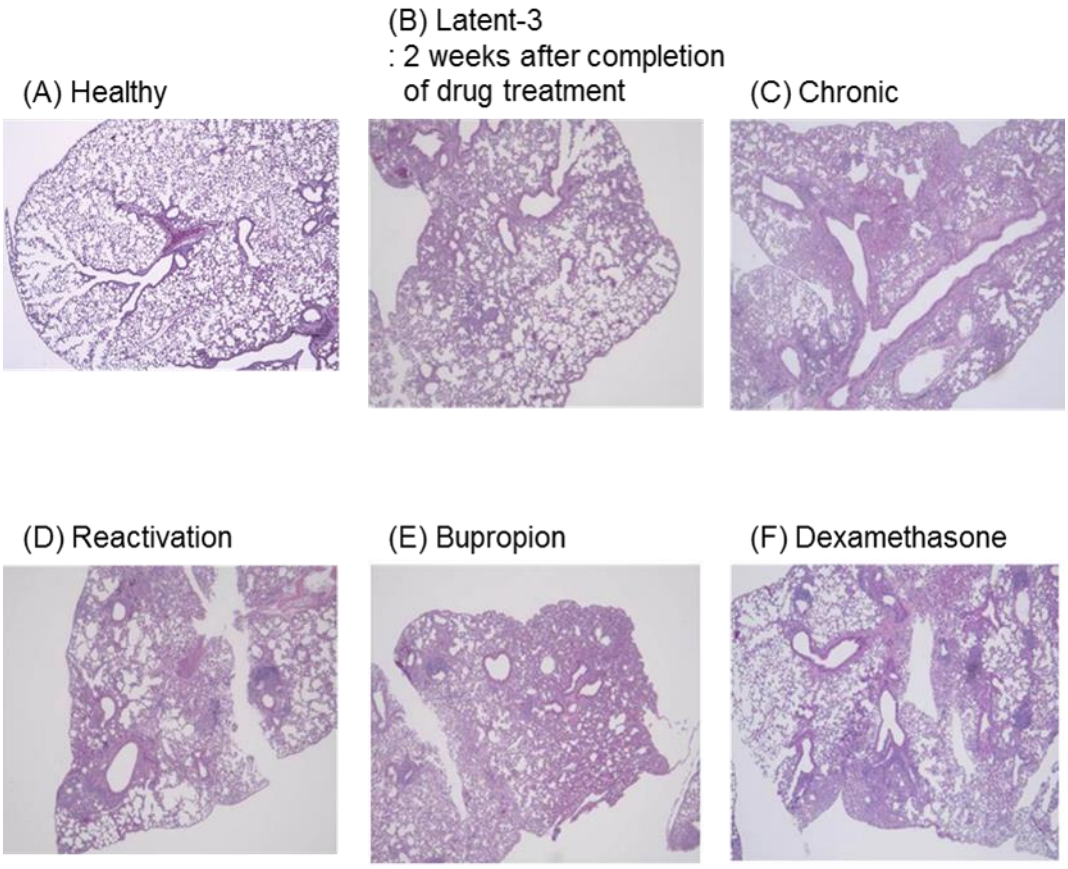

Figure 2. Histopathological findings. One lobe of the lungs was fixed in phosphate-buffered formaldehyde and embedded in paraffin. Sections were stained with haematoxylin and eosin. Acid-fast *M. tuberculosis* bacilli in the lung tissue were detected by Ziehl-Neelsen staining. The stained slides were observed under a light microscope (A-F, ×40 magnification).

2. Cytokine detection

A. Differentially-expressed genes among healthy, latent TB, and chronic TB infection mice

Of the genes expressed commonly among the healthy control, latent TB, and chronic TB mice, the cytokine profile was examined to identify the most significant potential marker genes that can distinguish between each type of infection status. A gene microarray was performed with total RNA isolated from the lung tissue, and three samples for each group of mice were processed (Figure 3A). The expression array we used can analyze 26,515 genes and 35,240 total RefSeq transcripts. After fold-change filtering (2-fold or greater difference in the gene expression level) and statistical filtering (p-value < 0.05 by the *t*-test), we analyzed the results using the Affymetrix Expression console 1.3.1, R program (3.0.2), and DAVID 6.7 software.

Compared to healthy mice, 114 and 577 genes were up-regulated in the LTBI and chronic TB mice, whereas 7 and 39 genes were down-regulated in the LTBI and chronic TB mice, respectively. A total of 205 genes showed increased expression common to both the LTBI and chronic TB groups, and 11 genes were common to the reduction (Figure 3B). Of the genes showing a common increase or decrease in expression in these groups, we selected immune-related genes that showed more than 2-fold difference in expression between the latent and chronic TB models and similar gene expression between healthy and latent TB mice. The number of genes that showed increased expression in the chronic stage compared to the latent stage are summarized in Table 1. In addition to these immune response genes, the other notably increased genes in the chronic stage were inducible nitric oxide synthase 2, matrix metallopeptidase 12, CD86, CD80, and molecules responsible for T cell activation such as CD3, CD6, lymphocyte-specific protein tyrosine kinase, interleukin-2-inducible T-cell kinase, and linker for activation of T cells. These immune response-related genes are summarized in

Table 2. This is because the main objective of this study was to identify genes expressed differentially between latent and chronic TB status, since these genes can be used along with the most urgently needed diagnostic method. A total of 17 immune-related genes (*Cxcl9, Cxcl10, Cxcl11, Ccl5, Ccl19, Ccl2, Ccl7, Ccl8, Ccl12, Il2rb, Il7r, Il12rb1, Il12rb2, Il21r, Il27r, Tnf*, and *Ifn-γ*) were ultimately selected and used to construct a heat map (Figure 3C). The three samples from the chronic phase of infection showed higher expression of these genes, than those of the latent phase and healthy mice.

(A)

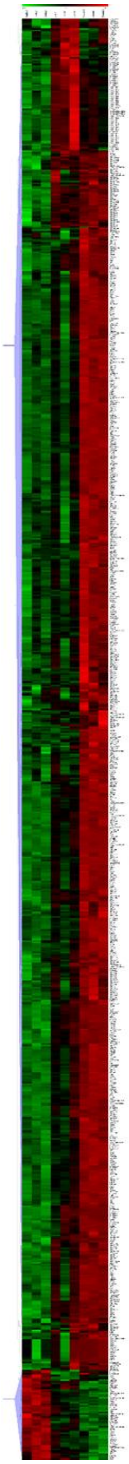

(B)

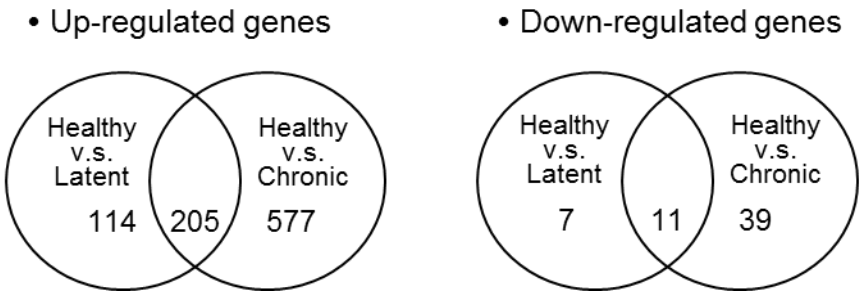

(C)

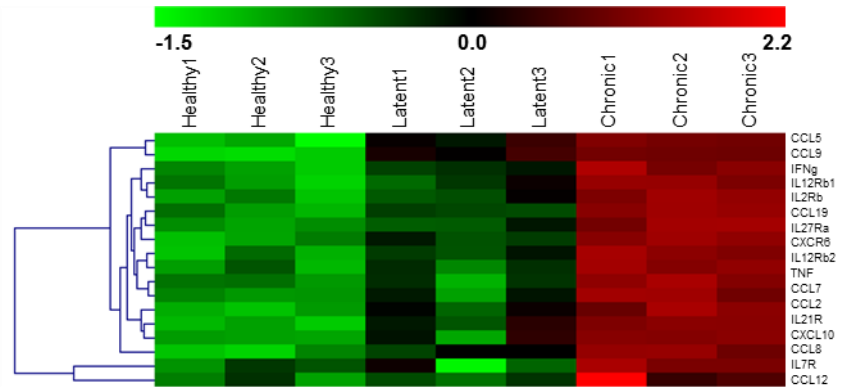

Figure 3. Differentially expressed genes in various infection stages of tuberculosis. Venn diagram of the differentially expressed genes in the lung tissues (B). Among the relative expression levels of total genes in the heat maps (A), we selected immune-related genes and then chose 17 immunological genes that showed differential expression between the stages of infection (C).

Table 1. Number of genes that showed increased expression in the chronic stage vs. the latent stage

Fold	Number
> 2	410
> 3	116
> 4	53
> 5	31

Table 2. List of immune response-related genes that were increased in the chronic stage compared to the latent stage

Chronic/Latent	Gene Symbol	Gene Description
5.9	Nos2	nitric oxide synthase 2, inducible
5.2	LOC630751	interferon-inducible GTPase 1-like
5.2	Ly6i	lymphocyte antigen 6 complex, locus I
4.2	Slamf8	signaling lymphocytic activation molecule family member 8
3.6	Tnf	tumor necrosis factor
3.6	Mmp12	matrix metallopeptidase 12
3.5	Cxcl10	chemokine (C-X-C motif) ligand 10
3.4	Cxcr6	chemokine (C-X-C motif) receptor 6
3.2	Ccr5	chemokine (C-C motif) receptor 5
3.1	Ccl8	chemokine (C-C motif) ligand 8
3.0	Xcr1	chemokine (C motif) receptor 1
2.8	Ifng	interferon gamma
2.8	Ccl19	chemokine (C-C motif) ligand 19
2.8	Slamf7	signaling lymphocytic activation molecule family member 7
2.7	Tnfrsf9	tumor necrosis factor receptor superfamily, member 9
2.7	Cd72	CD72 antigen
2.7	Fcgr1	Fc receptor, IgG, high affinity I
2.7	Ccl7	chemokine (C-C motif) ligand 7
2.6	Cxcl9	chemokine (C-X-C motif) ligand 9
2.6	Cd86	CD86 antigen
2.5	Cd3e	CD3 antigen, epsilon polypeptide
2.5	Mmp13	matrix metallopeptidase 13
2.5	Cd4	CD4 antigen
2.5	Ccl2	chemokine (C-C motif) ligand 2
2.4	Msr1	macrophage scavenger receptor 1
2.4	Cd3g	CD3 antigen, gamma polypeptide
2.4	Cd80	CD80 antigen
2.4	Gm2023	predicted gene 2023/ chemokine (C-C motif) ligand 19
2.4	Cd6	CD6 antigen
2.4	Cxcl11	chemokine (C-X-C motif) ligand 11
2.3	Ctss	cathepsin S
2.3	Ccl19	chemokine (C-C motif) ligand 19
2.3	Cd68	CD68 antigen
2.3	Cxcl5	chemokine (C-X-C motif) ligand 5
2.3	Lck	lymphocyte protein tyrosine kinase
2.2	Ly9	lymphocyte antigen 9
2.2	Slamf6	signaling lymphocytic activation molecule family member 6
2.2	Socs1	suppressor of cytokine signaling 1
2.2	Itk	IL2 inducible T cell kinase
2.2	Ccl19	chemokine (C-C motif) ligand 19
2.2	Ccl19	chemokine (C-C motif) ligand 19
2.2	Cd5	CD5 antigen
2.2	Cd40lg	CD40 ligand
2.1	Ccl20	chemokine (C-C motif) ligand 20
2.1	Cd52	CD52 antigen
2.1	Cd8b1	CD8 antigen, beta chain 1
2.1	Il23r	interleukin 23 receptor
2.1	Slamf9	signaling lymphocytic activation molecule family member 9
2.1	Ccl12	chemokine (C-C motif) ligand 12
2.0	Cxcr3	chemokine (C-X-C motif) receptor 3
2.0	Il21r	interleukin 21 receptor
2.0	Lat	linker for activation of T cells

B. Analysis of tissue RNA profiles

We classified the 17 genes that showed differential expression between the groups into four main categories. The first category included the chemokines excluding MCPs such as *Cxcl9, Cxcl10, Cxcl11, Ccl5, Ccl19*. *CXCL9, CXCL10*, and *CXCL11* are already established as human TB biomarkers (Figure 4A). The second category included the MCPs encoding monocyte chemoattractant protein (MCP) such as *Ccl2, Ccl7, Ccl8*, and *Ccl12 (*Figure 4B). The third category included receptors such as *Il2rb*, *Il7r, Il12rb1, Il12rb2, Il21r*, and *Il27r* (Figure 4C). The last category included *Tnf* and *Ifn-γ* (Figure 4D). Expression data obtained by microarray analysis and real-time PCR are summarized in Table 3, showing the fold change and p-value obtained in the comparison of chronic versus latent TB. The data for the comparison of latent TB versus healthy, and the comparison of chronic TB versus healthy are summarized in Table 4. Similar results were obtained with RT-qPCR and the microarray data, although there was not a complete match.

(A)

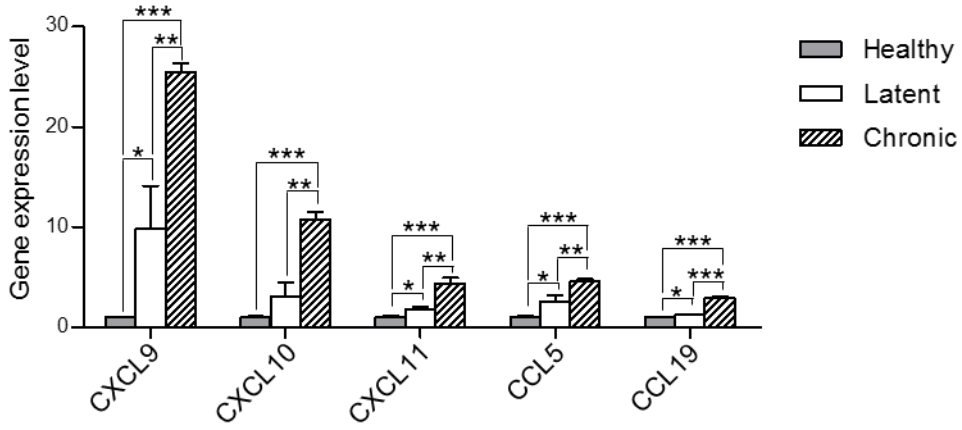

(B)

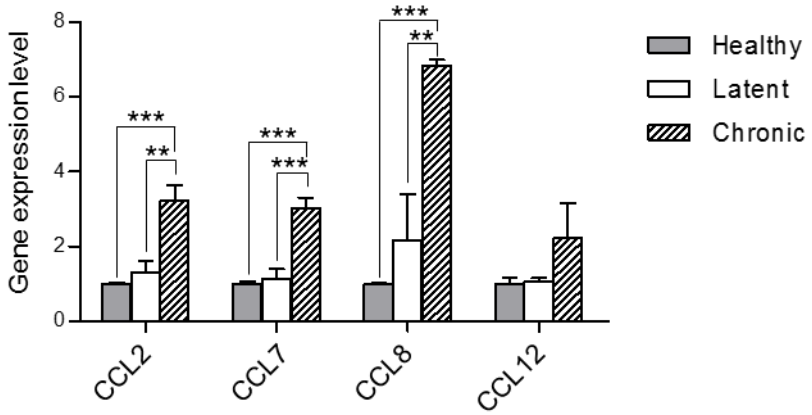

(C)

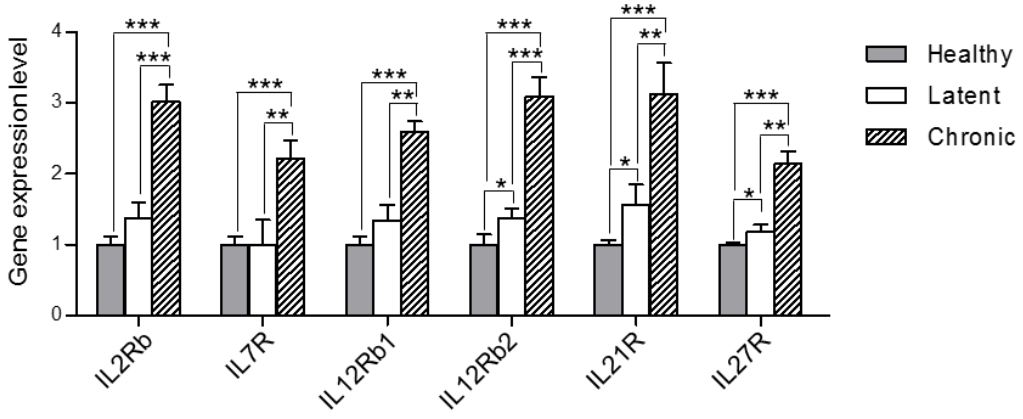

(D)

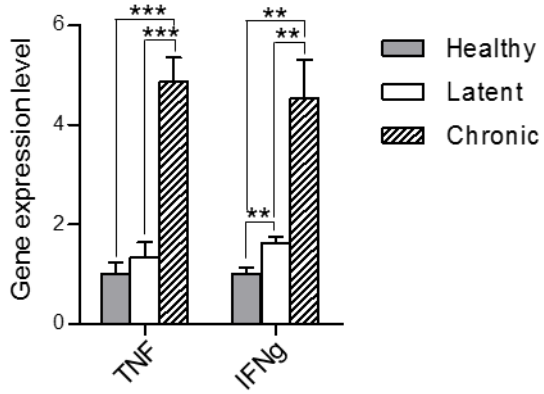

Figure 4. cDNA microarray analysis of 17 genes showing differential expression among TB infection stages. Microarray analysis of mature miRNA levels. Fold changes in mature miRNA levels are shown relative to the control. Chemokines excluding MCPs (A), MCPs (B), receptors (C), TNF and IFN-γ (D). Error bars indicate the standard deviation. Student's t-tests were performed; statistically significant results are marked with * ($p < 0.05$); ** ($p < 0.01$); *** ($p < 0.001$); ns: not significant ($p > 0.05$).

Table 3. Statistical analysis of data obtained by microarray and RT-qPCR (chronic vs. latent)

Gene		Microarrays		RT-qPCR	
		Fold change	P-value	Fold change	P-value
Chemokine excluding MCPs	CXCL9	2.59	0.0035	7.20	0.0067
	CXCL10	3.55	0.0011	4.84	0.0162
	CXCL11	2.37	0.0022	3.91	0.0464
	CCL5	1.81	0.0052	2.72	0.0008
	CCL19	2.32	<0.0001	4.16	0.0008
MCPs	CCL2	2.47	0.0031	4.24	0.0069
	CCL7	2.66	0.0010	5.16	0.0029
	CCL8	3.14	0.0029	3.78	0.0094
	CCL12	2.06	0.1064	5.25	0.0081
Receptors	IL2Rβ	2.20	0.0009	3.14	0.0076
	IL7R	2.21	0.0078	2.35	0.0370
	IL12Rβ1	1.93	0.0012	5.24	0.0249
	IL12Rβ2	2.26	0.0006	3.00	0.0219
	IL21R	2.00	0.0069	1.92	0.0379
	IL27Rα	1.81	0.0012	3.37	0.0371
TNF and IFN-γ	TNF	3.61	0.0004	2.41	0.2679
	IFN-γ	2.80	0.0032	2.63	0.0405

Table 4. Statistical analysis of data obtained by microarray and RT-qPCR (latent vs. healthy and chronic vs. healthy)

Gene		Microarrays				RT-qPCR			
		Latent/healthy		Chronic/healthy		Latent/healthy		Chronic/healthy	
		Fold change	P-value	Fold change	P-value	Fold change	P-value	Fold change	P-value
Chemokine excluding MCPs	CXCL9	9.83	0.0236	25.44	<0.0001	41.85	0.0176	301.26	0.0036
	CXCL10	3.04	0.0693	10.78	<0.0001	3.70	0.0189	17.90	0.0084
	CXCL11	1.85	0.0102	4.38	0.0006	1.56	0.4692	6.10	0.0328
	CCL5	2.55	0.0131	4.62	<0.0001	2.29	0.0420	6.23	0.0006
	CCL19	1.26	0.0146	2.92	<0.0001	1.07	0.7142	4.46	0.0007
MCPs	CCL2	1.30	0.1675	3.22	0.0008	0.99	0.4698	4.19	0.0078
	CCL7	1.14	0.4095	3.03	0.0003	1.78	0.1474	9.17	0.0024
	CCL8	2.18	0.1727	6.83	<0.0001	7.21	0.0179	27.26	0.0028
	CCL12	1.08	0.4760	2.22	0.0929	1.11	0.8058	5.83	0.0089
Receptors	IL2Rβ	1.38	0.0620	3.02	0.0002	0.83	0.5622	2.59	0.0157
	IL7R	1.00	0.9932	2.22	0.0016	1.07	0.8294	2.53	0.0388
	IL12Rβ1	1.35	0.0757	2.59	0.0001	2.16	0.0661	11.33	0.0167
	IL12Rβ2	1.37	0.0321	3.10	0.0003	0.95	0.8982	2.84	0.0438
	IL21R	1.56	0.0284	3.12	0.0012	1.91	0.1124	5.48	0.0156
	IL27Rα	1.18	0.0385	2.14	0.0004	0.59	0.1090	2.00	0.0988
TNF and IFN-γ	TNF	1.35	0.1865	4.86	0.0003	1.85	0.2775	4.46	0.1649
	IFN-γ	1.61	0.0054	4.52	0.0016	2.29	0.2260	6.02	0.0533

C. Validation of the microarray data

RT-qPCR analysis of genes from the lung tissues was employed to validate the microarray data. The gene expression patterns of the 17 candidate markers were selected to evaluate whether they could be used to discriminate between latent TB and chronic TB infection. The expression levels of the selected genes were calculated relative to the level of the housekeeping gene *gapdh*. The primer sequences used for RT-qPCR and additional information are shown in Table 5. The genes were divided into the same four categories described above (chemokines excluding MCPs, Figure 5A; MCPs, Figure 5B; receptors, Figure 5C; *Tnf* and *Ifn-γ*, Figure 5D). In particular, mRNA expression levels of *Cxcl9, Ccl7* and *Ccl12* were significantly higher in chronic TB than latent TB, indicating that these cytokines could be used to distinguish latent TB from chronic TB. And *Ccl2, Ccl7, Ccl8*, and *Ccl12* respectively encode MCP1, MCP3, MCP2, and MCP5, indicating a significant role of macrophages in the chronic stage and these also showed potential as sensitive and effective markers. Each of these genes could serve as a single candidate for the detection of chronic TB, but the combination of candidates might serve as an even more specific biomarker.

(A)

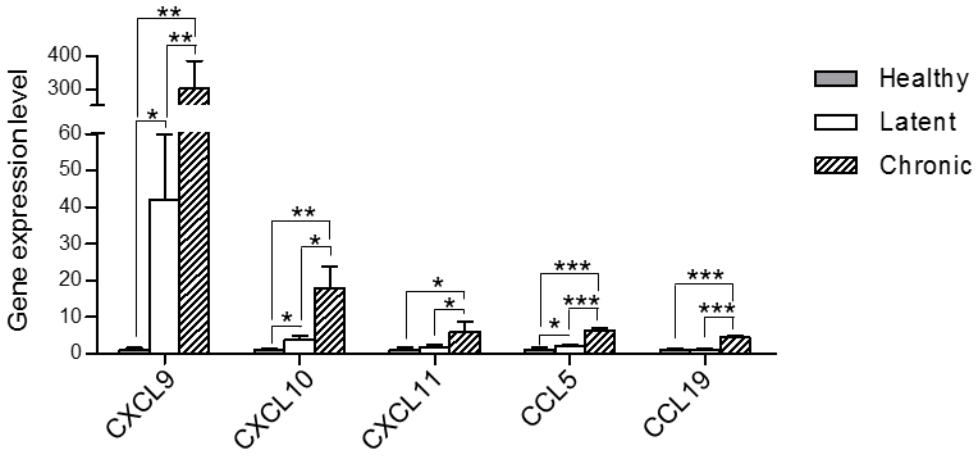

(B)

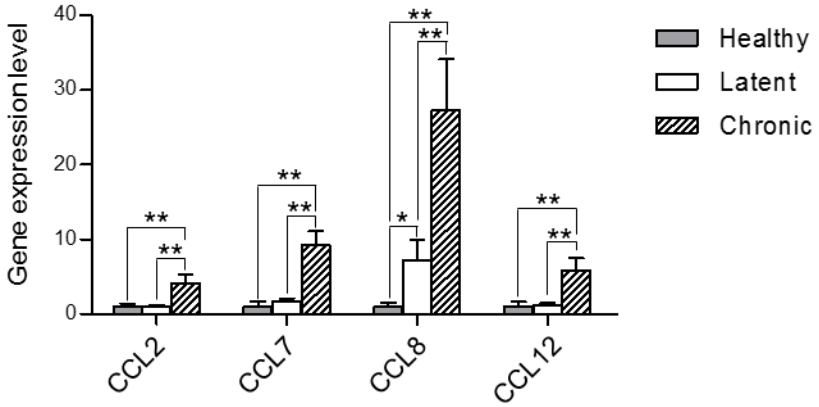

(C)

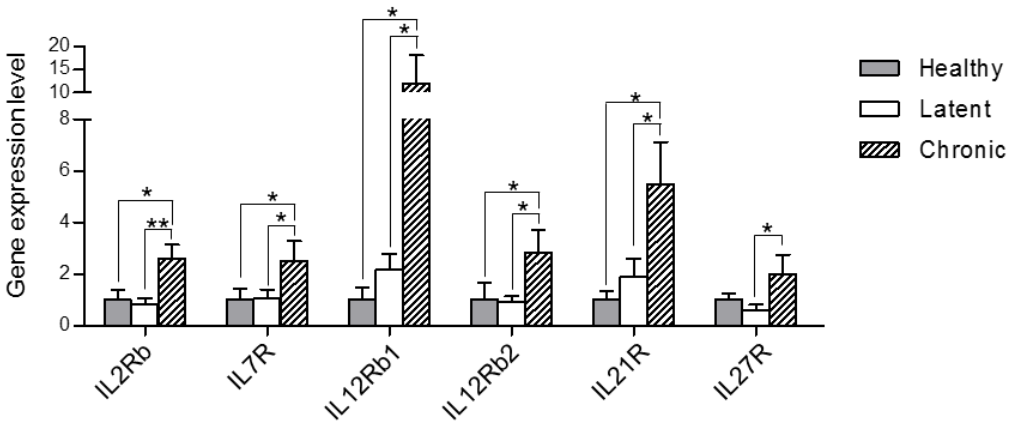

(D)

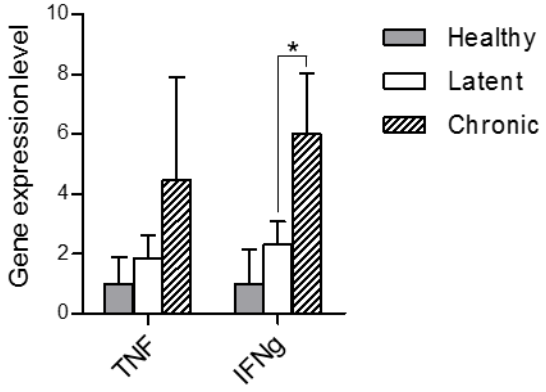

Figure 5. RT-qPCR analysis of 17 genes showing differential expression among TB infection stages. RT-qPCR analysis of mature miRNA levels. Fold changes in mature miRNA levels are shown relative to the control. Chemokines excluding MCPs (A), MCPs (B), receptors (C), TNF and IFN-γ (D). Error bars indicate the standard deviation. Student's t-tests were performed; statistically significant results are marked with * ($p < 0.05$); ** ($p < 0.01$); *** ($p < 0.001$); ns: not significant ($p > 0.05$).

Table 5. RT-qPCR primer sequences

Gene description	Gene symbol	Primer sequence (5'-3') Forward & Reverse	Sequence accession number
Chemokine (C-X-C motif) ligand 9	CXCL9	AGT CCG CTG TTC TTT TCC TC TGA GGT CTT TGA GGG ATT TGT AG	NM_008599
Chemokine (C-X-C motif) ligand 10	CXCL10	TCA GCA CCA TGA ACC CAA G CTA TGG CCC TCA TTC TCA CTG	NM_021274
Chemokine (C-X-C motif) ligand 11	CXCL11	ATG GCA GAG ATC GAG AAA GC TGC ATT ATG AGG CGA GCT TG	NM_019494
Chemokine (C-C motif) ligand 5	CCL5	GGG TAC CAT GAA GAT CTC TGC TCT AGG GAG AGG TAG GCA AAG	NM_013653
Chemokine (C-C motif) ligand 19	CCL19	AGA CTG CTG CCT GTC TGT GA GCC TTT GTT CTT GGC AGA AG	NM_011888
Chemokine (C-C motif) ligand 2	CCL2	CAT CAG TCC TCA GGT ATT GGC TTG TGA TTC TCC TGT AGC TCT TC	NM_011333
Chemokine (C-C motif) ligand 7	CCL7	TCT CTC ACT CTC TTT CTC CAC C GGG ATC TTT TGT TTC TTG ACA TAG C	NM_013654
Chemokine (C-C motif) ligand 8	CCL8	ACA ATA TCC AGT GCC CCA TG CAT GTA CTC ACT GAC CCA CTT C	NM_021443
Chemokine (C-C motif) ligand 12	CCL12	CAT CAG TCC TCA GGT ATT GGC TTG TGA TTC TCC TGT AGC TCT TC	NM_011331
Interleukin 2 receptor, beta chain	IL2Rβ	GGT TGG CGT AGG GTA AAG AC CAG AAC TTG GAG GGA ATG AGG	NM_008368
Interleukin 7 receptor	IL7R	TCT GGA GAA AGT GGA AAT GCC AGC TGT GTT GAT GTC TGA GTC	NM_008372
Interleukin 12 receptor, beta 1	IL12Rβ1	CCA GCA AAC ACA TCA CCT TC TGG AAA CCC TGT AGC AAC TC	NM_008353
Interleukin 12 receptor, beta 2	IL12Rβ2	GAA CGC CTT TTC ATT TCC TGG TGG ATG TGA GTT TTG AGA GCG	NM_008354
Interleukin 21 receptor	IL21R	GCT TAT GAC GAA CCC TCC AAC ACG TTT CTT GAG TCC ACT GAG	NM_021887
Interleukin 27 receptor, alpha	IL27Rα	CCA GAC GCC ATT CTT AGA TCC TAA TAT CTC CAG CCC CAA ACC	NM_016671
Tumor necrosis factor	TNF	AGG GAT GAG AAG TTC CCA AAT G GGC TTG TCA CTC GAA TTT TGA GA	NM_001278601
Interferon gamma	IFN-γ	TTT AAC TCA AGT GGC ATA GAT GTG G TGC AGG ATT TTC ATG TCA CCA T	NM_008337

D. Analysis of serum protein profiles

Based on the mRNA-level in the lung tissue, the direct effects from TB infection were identified according to the changes of expression of the immune-related genes. More importantly, it is crucial to determine whether these genetic changes also affect protein expression. The ultimate goal of TB diagnosis is to find a fast, accurate, and easy method of diagnosis so that if the genetic changes in blood and lesions are consistent, it will be the most accurate diagnostic standard.

As previously confirmed by microarray and real-time PCR, CCL7 and CCL12 are considered candidates for efficient biomarkers. Luminex was performed to confirm whether they have the same tendency in the protein level of the serum of the infected mouse. Each infection stage; healthy (n = 6), latent (n = 3) and chronic (n = 3), both CCL7 and CCL12 showed higher expression levels in chronic than in latent, but did not find meaningful results.

(A) CCL7

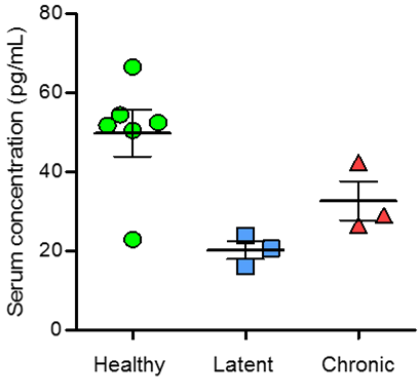

(B) CCL12

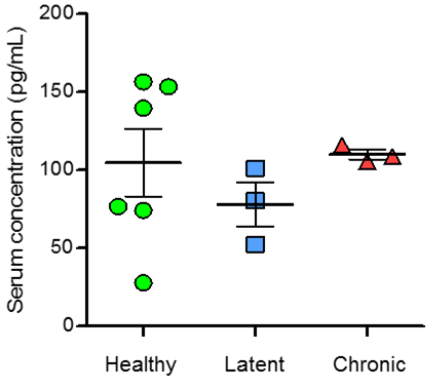

Figure 6. Detection of CCL7 and CCL12 in serum. Protein expression of CCL7 and CCL12 in MCPs was confirmed by using the serum from TB infected mice.

3. MiRNA detection

A. Differentially expressed genes among healthy, latent TB, chronic TB, spontaneous reactivation and bupropion/dexamethasone treatment mice

In addition to healthy control, latent and chronic TB mice and, spontaneous reactivation and bupropion/dexamethasone (immunosuppressant) treatment mice were used to confirm the expression of microRNAs in each infection stage. MicroRNAs can specifically detect the gene marker of TB more specifically than the cytokines and chemokines mentioned above because they specifically regulate gene expression.

A gene microarray was performed with total RNA containing microRNA isolated from the lung tissue, and three samples for each group of mice were processed (Figure 7A). The expression array can analyze mouse mature miRNA probe sets containing 1,908 genes and total miRNA probe sets containing 30,434 genes. After fold-change filtering (1.5-fold or greater difference in the gene expression level) and statistical filtering (p-value < 0.05 by the *t*-test), we analyzed the results using Affymetrix GeneChip Mouse miRNA 4.0 Array x 12.

Compared to healthy mice, 55 miRNAs were increased and 81 miRNAs were decreased in latent, chronic TB, and reactivation mice (Figure 7B). 26 miRNAs were selected from the genes that showed more than 1.5-fold difference in expression among each stage (Figure 7C). A list of differentially expressed miRNAs in the latent, chronic TB, reactivation compared to the healthy mice are summarized in Table 6, based on healthy, the increase was yellow and the decrease was blue. The targets of mmu-miR-675-3p, mmu-miR-450b-3p presented in the database are summarized in Table 7, 8.

(A)

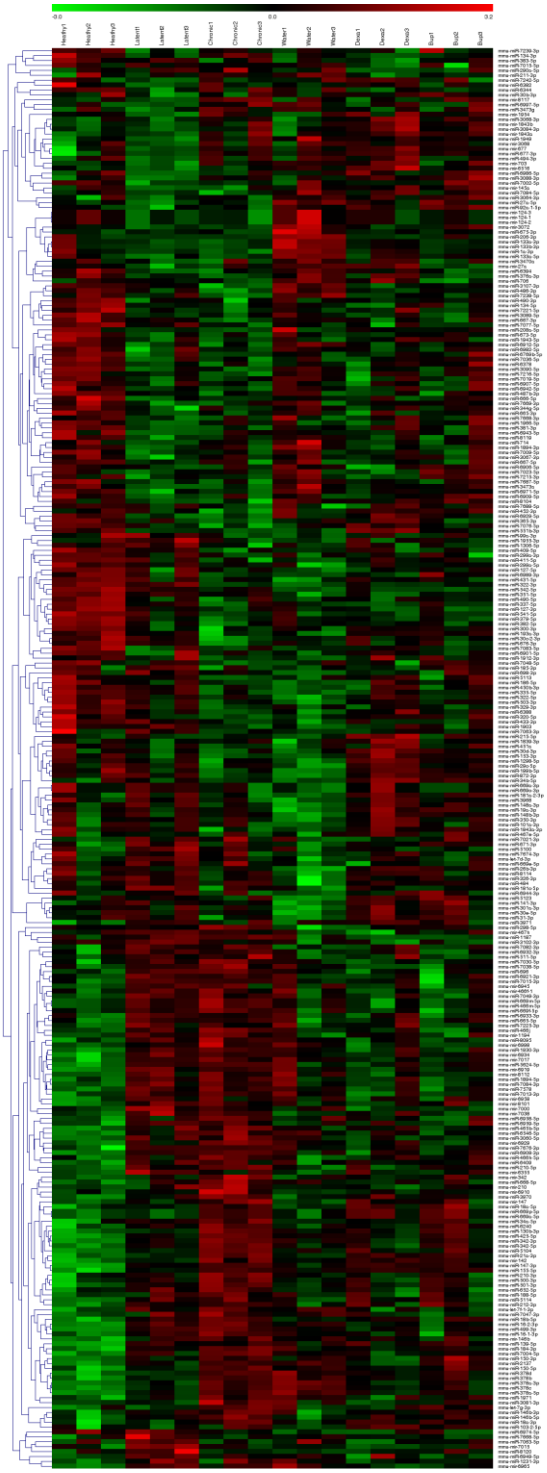

(B)

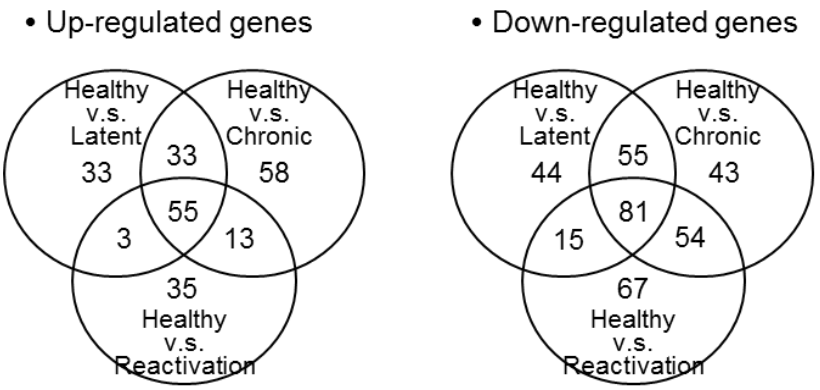

(C)

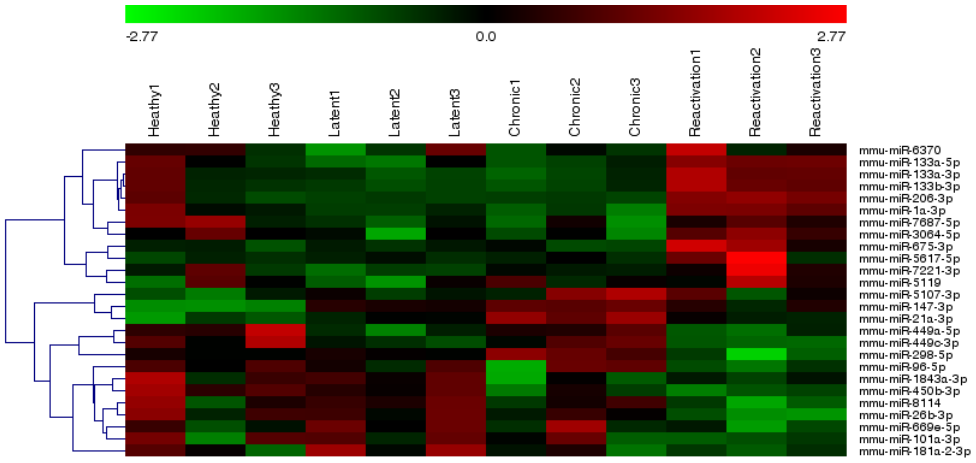

Figure 7. Differentially expressed microRNAs depending on infection stages of mice. Heat map of differentially expressed genes of healthy, latent TB, chronic TB, spontaneous reactivation and bupropion/dexamethasone treatment mice lung tissues (A). Among genes described in Venn diagram that showed increased/decreased gene expression in the spontaneous reactivation stage vs. chronic stage vs. the latent stage (B), 26 miRNAs were selected (C).

Table 6. List of significantly differentially expressed 26 miRNAs in the latent, chronic TB, and spontaneous reactivation mice compared to the healthy mice

Latent	Chronic	Reactivation	Transcript ID(Array Design)	Accession
1.8	5.5	1.8	mmu-miR-21a-3p	MIMAT0004628
22.9	79.9	19.5	mmu-miR-147-3p	MIMAT0004857
2.9	4.1	1.9	mmu-miR-1a-3p	MIMAT0000123
4.2	4.4	2.9	mmu-miR-133a-5p	MIMAT0003473
2.2	2.2	2.4	mmu-miR-133a-3p	MIMAT0000145
89.9	90.1	13.4	mmu-miR-206-3p	MIMAT0000239
2.2	2.1	2.6	mmu-miR-133b-3p	MIMAT0000769
1.9	2.2	1.5	mmu-miR-3064-5p	MIMAT0014834
1.7	4.1	6.8	mmu-miR-450b-3p	MIMAT0003512
3.5	3.6	1.5	mmu-miR-7687-5p	MIMAT0029902
1.4	3.7	1.9	mmu-miR-5107-3p	MIMAT0022985
1.0	1.6	1.7	mmu-miR-298-5p	MIMAT0000376
1.1	1.5	1.5	mmu-miR-6370	MIMAT0025114
1.1	1.8	6.7	mmu-miR-26b-3p	MIMAT0004630
1.3	3.5	2.7	mmu-miR-1843a-3p	MIMAT0014806
1.9	1.3	1.7	mmu-miR-181a-2-3p	MIMAT0005443
1.6	1.4	1.5	mmu-miR-669e-5p	MIMAT0005853
1.5	1.1	1.6	mmu-miR-5119	MIMAT0020627
1.6	1.2	1.8	mmu-miR-7221-3p	MIMAT0028411
2.6	1.4	2.8	mmu-miR-449a-5p	MIMAT0001542
3.0	1.3	4.3	mmu-miR-449c-3p	MIMAT0022715
1.1	1.0	3.0	mmu-miR-675-3p	MIMAT0003726
1.2	1.2	4.7	mmu-miR-5617-5p	MIMAT0022361
1.0	1.3	2.9	mmu-miR-101a-3p	MIMAT0000133
1.3	1.0	3.1	mmu-miR-96-5p	MIMAT0000541
1.0	1.5	3.9	mmu-miR-8114	MIMAT0031420

Table 7. Targets of mmu-miR-675-3p

Gene Symbol	Description	Transcript ID
Cdk13	cyclin-dependent kinase 13	NM_001081058
Cdk13	cyclin-dependent kinase 13	NM_027118
Synpr	synaptoporin	NM_028052
Atg4a	autophagy-related 4A (yeast)	NM_174875
Cyld	cylindromatosis (turban tumor syndrome)	NM_001128169
Cyld	cylindromatosis (turban tumor syndrome)	NM_001128171
Chek1	checkpoint kinase 1 homolog (S. pombe)	NM_007691
Synpr	synaptoporin	NM_001163032
Elf1	E74-like factor 1	NM_007920
Smek1	SMEK homolog 1, suppressor of mek1 (Dictyostelium)	NM_001160214
Klhl1	kelch-like 1 (Drosophila)	NM_053105
Pitx2	paired-like homeodomain transcription factor 2	NM_001042504
Pitx2	paired-like homeodomain transcription factor 2	NM_011098
Setd8	SET domain containing (lysine methyltransferase) 8	NM_030241
Cyld	cylindromatosis (turban tumor syndrome)	NM_173369
Zfp711	zinc finger protein 711	NM_177747
Pitx2	paired-like homeodomain transcription factor 2	NM_001042502
Unc13c	unc-13 homolog C (C. elegans)	NM_001081153
Cyld	cylindromatosis (turban tumor syndrome)	NM_001128170
Smek1	SMEK homolog 1, suppressor of mek1 (Dictyostelium)	NM_211355
Stk39	serine/threonine kinase 39, STE20/SPS1 homolog (yeast)	NM_016866

Table 8. Targets of mmu-miR-450b-3p

Gene Symbol	Description	Transcript ID
Srsf5	serine/arginine-rich splicing factor 5	NM_009159
Abcf3	ATP-binding cassette, sub-family F (GCN20), member 3	NM_013852
Olfm1	olfactomedin 1	NM_001038612
Gprasp2	G protein-coupled receptor associated sorting protein 2	NM_001163015
Pias3	protein inhibitor of activated STAT 3	NM_001165949
Ctnna1	catenin (cadherin associated protein), alpha 1	NM_009818
Cngb3	cyclic nucleotide gated channel beta 3	NM_013927
Tmem200a	transmembrane protein 200A	NM_029881
Tox	thymocyte selection-associated high mobility group box	NM_145711
Srsf5	serine/arginine-rich splicing factor 5	NM_001079695
Frmpd4	FERM and PDZ domain containing 4	NM_001033330
Fga	fibrinogen alpha chain	NM_010196
Mkrn1	makorin, ring finger protein, 1	NM_018810
Olfm1	olfactomedin 1	NM_001038614
Srsf5	serine/arginine-rich splicing factor 5	NM_001079694
Snn	stannin	NM_009223
Rab14	RAB14, member RAS oncogene family	NM_026697
Eny2	enhancer of yellow 2 homolog (Drosophila)	NM_175009
Sim1	single-minded homolog 1 (Drosophila)	NM_011376
Best1	bestrophin 1	NM_011913
Zeb2	zinc finger E-box binding homeobox 2	NM_015753
Tmed7	transmembrane emp24 protein transport domain containing 7	NM_025698
Ppip5k1	diphosphoinositol pentakisphosphate kinase 1	NM_178795
Gprasp2	G protein-coupled receptor associated sorting protein 2	NM_001163016
Pias3	protein inhibitor of activated STAT 3	NM_146135
Fam100b	family with sequence similarity 100, member B	NM_176902
Gprasp2	G protein-coupled receptor associated sorting protein 2	NM_001163017
Cdh2	cadherin 2	NM_007664
Pias3	protein inhibitor of activated STAT 3	NM_018812

B. Analysis of tissue microRNA profiles

The microarray data (Figure 8A, B) shows the 10 targets selected (mmu-miR-1a-3p, mmu-miR-133a-5p, mmu-miR-133a-3p, mmu-miR-206-3p, mmu-miR-133b-3p, mmu-miR-3064-5p, mmu-miR-450b-3p, mmu-miR-26b-3p, mmu-miR-181a-2-3p, mmu-miR-8114) from the 26 miRNAs. It is suggested in the paper that mmu-miR-1a-3p and mmu-miR-206-3p can distinguish healthy people from active TB patients. Unlike human, in the case of mice, mmu-miR-1a-3p and mmu-miR-206-3p were found to be appropriate markers to distinguish between latent and spontaneous reactivation. Since mmu-miR-206-3p rarely expresses in latent and active groups, spontaneous reactivation can be more clearly distinguished. Since miRNAs are present in much smaller amounts than genes expressed in proteins, it is difficult to judge the infecting stage of tuberculosis by comparing the amount of miRNA. Therefore, if promising targets are combined, they may be able to distinguish healthy, latent, chronic, and reactivation mice at the same time. Statistical analysis of data obtained by microarray and RT-qPCR (reactivation vs. latent) are summarized in Table 9 and statistical analysis of data obtained by microarray and RT-qPCR (latent vs. healthy, chronic vs. healthy and reactivation vs. healthy) are summarized in Table 10, 11. miRNA information are summarized in Table 12.

(A)

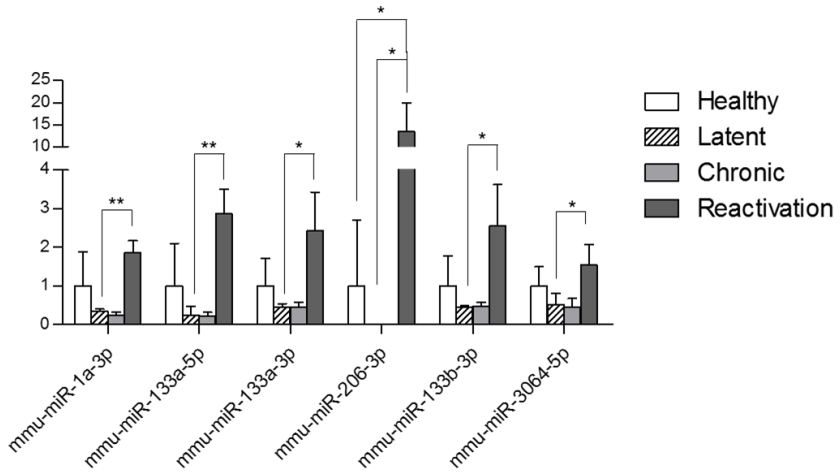

(B)

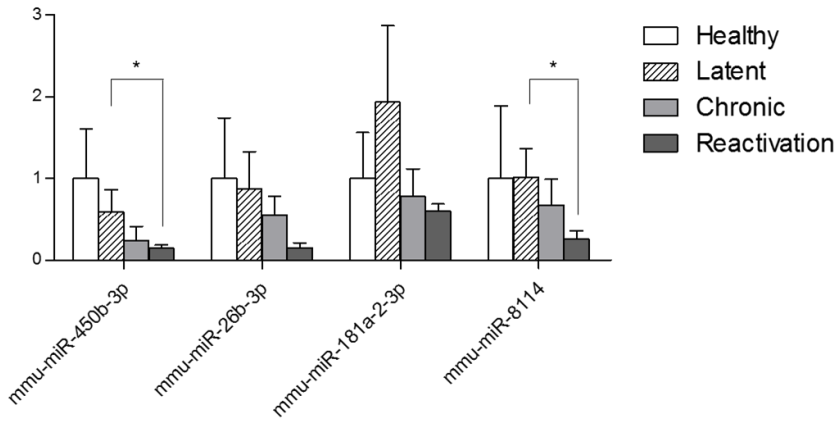

Figure 8. Microarray analysis of 10 microRNAs in tissues showing differential expression among TB infection stages. Microarray analysis of mature miRNA levels. Fold changes in mature miRNA levels are shown relative to the control. Error bars indicate the standard deviation. Student's t-tests were performed; statistically significant results are marked with * ($p < 0.05$); ** ($p < 0.01$); *** ($p < 0.001$); ns: not significant ($p > 0.05$).

Table 9. Statistical analysis of data obtained by microarray and RT-qPCR (reactivation vs. latent)

Gene	Microarrays		RT-qPCR	
	Fold change	P-value	Fold change	P-value
mmu-miR-1a-3p	5.38	0.0012	5.36	0.0059
mmu-miR-133a-5p	11.96	0.0028	5.73	0.1879
mmu-miR-133a-3p	5.29	0.0276	12.19	0.0105
mmu-miR-206-3p	1206.87	0.0232	4304.35	0.0123
mmu-miR-133b-3p	5.61	0.0273	8.05	0.0255
mmu-miR-3064-5p	2.92	0.0450	2.05	0.0623
mmu-miR-450b-3p	0.25	0.0478	1.33	0.4075
mmu-miR-26b-3p	0.17	0.0504	0.94	0.8383
mmu-miR-181a-2-3p	0.31	0.0692	0.98	0.9697
mmu-miR-8114	0.25	0.0230	1.02	0.9471

Table 10. Statistical analysis of data obtained by microarray (latent vs. healthy, chronic vs. healthy and reactivation vs. healthy)

Gene	Microarrays					
	Latent/healthy		Chronic/healthy		Reactivation/healthy	
	Fold change	P-value	Fold change	P-value	Fold change	P-value
mmu-miR-1a-3p	0.34	0.2709	0.24	0.2146	1.86	0.1901
mmu-miR-133a-5p	0.24	0.3048	0.23	0.2911	2.87	0.0641
mmu-miR-133a-3p	0.46	0.2649	0.46	0.2683	2.42	0.1159
mmu-miR-206-3p	0.01	0.3719	0.01	0.3719	13.42	0.0327
mmu-miR-133b-3p	0.46	0.2906	0.48	0.3118	2.55	0.1112
mmu-miR-3064-5p	0.53	0.2309	0.45	0.1619	1.54	0.2735
mmu-miR-450b-3p	0.59	0.3468	0.24	0.1058	0.15	0.0714
mmu-miR-26b-3p	0.88	0.8178	0.55	0.3750	0.15	0.1180
mmu-miR-181a-2-3p	1.93	0.2111	0.78	0.5862	0.60	0.2895
mmu-miR-8114	1.01	0.9801	0.68	0.5821	0.26	0.2222

Table 11. Statistical analysis of data obtained by RT-qPCR (latent vs. healthy, chronic vs. healthy and reactivation vs. healthy)

Gene	RT-qPCR					
	Latent/healthy		Chronic/healthy		Reactivation/healthy	
	Fold change	P-value	Fold change	P-value	Fold change	P-value
mmu-miR-1a-3p	0.49	0.4223	0.26	0.2519	2.64	0.0689
mmu-miR-133a-5p	0.29	0.2322	0.23	0.1994	2.47	0.5504
mmu-miR-133a-3p	0.27	0.2637	0.20	0.2256	3.33	0.0561
mmu-miR-206-3p	0.01	0.2878	0.00	0.2863	24.72	0.0147
mmu-miR-133b-3p	0.29	0.2597	0.20	0.2154	2.31	0.1758
mmu-miR-3064-5p	1.14	0.3121	0.90	0.3538	2.34	0.0410
mmu-miR-450b-3p	0.75	0.3189	0.44	0.0333	0.99	0.9852
mmu-miR-26b-3p	0.92	0.6675	0.39	0.0025	0.87	0.5215
mmu-miR-181a-2-3p	0.37	0.0174	0.39	0.0289	0.36	0.0546
mmu-miR-8114	0.89	0.6607	0.54	0.0823	0.91	0.6249

Table 12. miRNA information

Transcript ID	Mature miRNA Sequence (5'-3')	Sequence accession number
mmu-miR-1a-3p	UGGAAUGUAAAGAAGUAUGUAU	MIMAT0000123
mmu-miR-133a-5p	GCUGGUAAAAUGGAACCAAAU	MIMAT0003473
mmu-miR-133a-3p	UUUGGUCCCCUUCAACCAGCUG	MIMAT0000145
mmu-miR-206-3p	UGGAAUGUAAGGAAGUGUGUGG	MIMAT0000239
mmu-miR-133b-3p	UUUGGUCCCCUUCAACCAGCUA	MIMAT0000769
mmu-miR-3064-5p	UCUGGCUGUUGUGGUGUGCAAA	MIMAT0014834
mmu-miR-450b-3p	AUUGGGAACAUUUUGCAUGCAU	MIMAT0003512
mmu-miR-26b-3p	CCUGUUCUCCAUUACUUGGCUC	MIMAT0004630
mmu-miR-181a-2-3p	ACCGACCGUUGACUGUACCUUG	MIMAT0005443
mmu-miR-8114	UCACCCAUCUCCUCUCCGCCU	MIMAT0031420

C. Validation of the microarray data

RT-qPCR was performed to confirm microarray data. RT-qPCR is considered to be more reliable than microarray. The gene expression patterns of the 10 candidate markers were selected to evaluate whether they could be used in discriminant among latent, chronic TB, and reactivation mice. As a result, mmu-miR-1a-3p could be an appropriate biomarker to distinguish all stages of infection. In addition, mmu-miR-206-3p is the target that best distinguishes spontaneous reactivation compared to health and latent. The expression levels of the selected genes were calculated relative to the level of the u6 (Figure 9A, B).

(A)

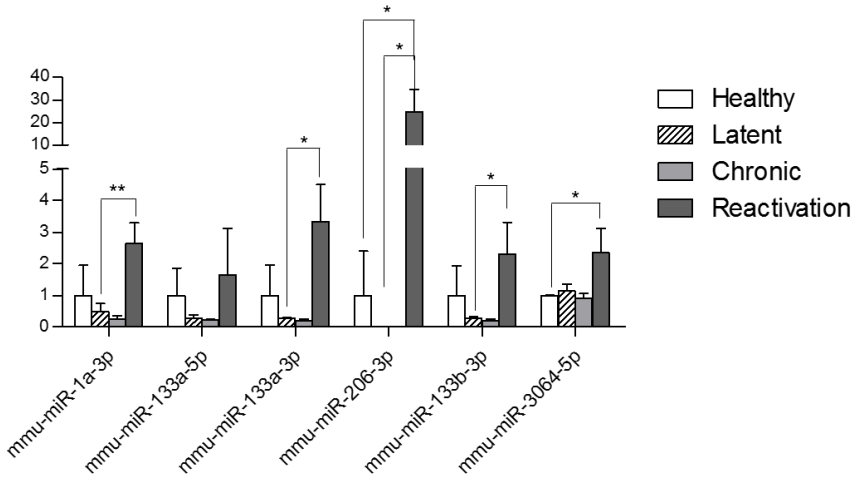

(B)

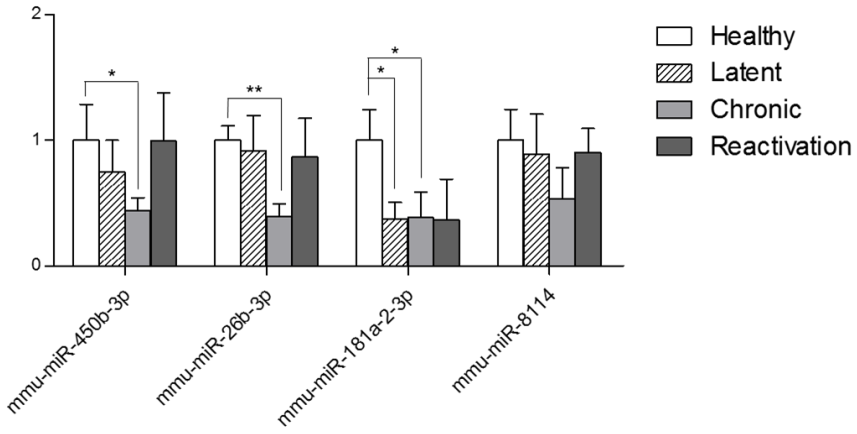

Figure 9. RT-qPCR analysis of 10 microRNAs in tissues showing differential expression among TB infection stages. RT-qPCR analysis of mature miRNA levels. Fold changes in mature miRNA levels are shown relative to the control. Error bars indicate the standard deviation. Student's t-tests were performed; statistically significant results are marked with * ($p < 0.05$); ** ($p < 0.01$); *** ($p < 0.001$); ns: not significant ($p > 0.05$).

D. Differentially expressed genes among spontaneous reactivation, bupropion/dexamethasone treatment mice model

Finally, to analyze the difference between spontaneous reactivation and immunosuppressant, microarrays were performed with miRNAs obtained from tissues of TB-infected mice. CFU or histological findings showed a similar degree of pathology, but different types of miRNAs are increasing or decreasing as shown in the heatmap results. If these are analyzed, it may be possible to analyze differences in drug mechanism or spontaneous reactivation and differences in between bupropion and dexamethasone.

(A)

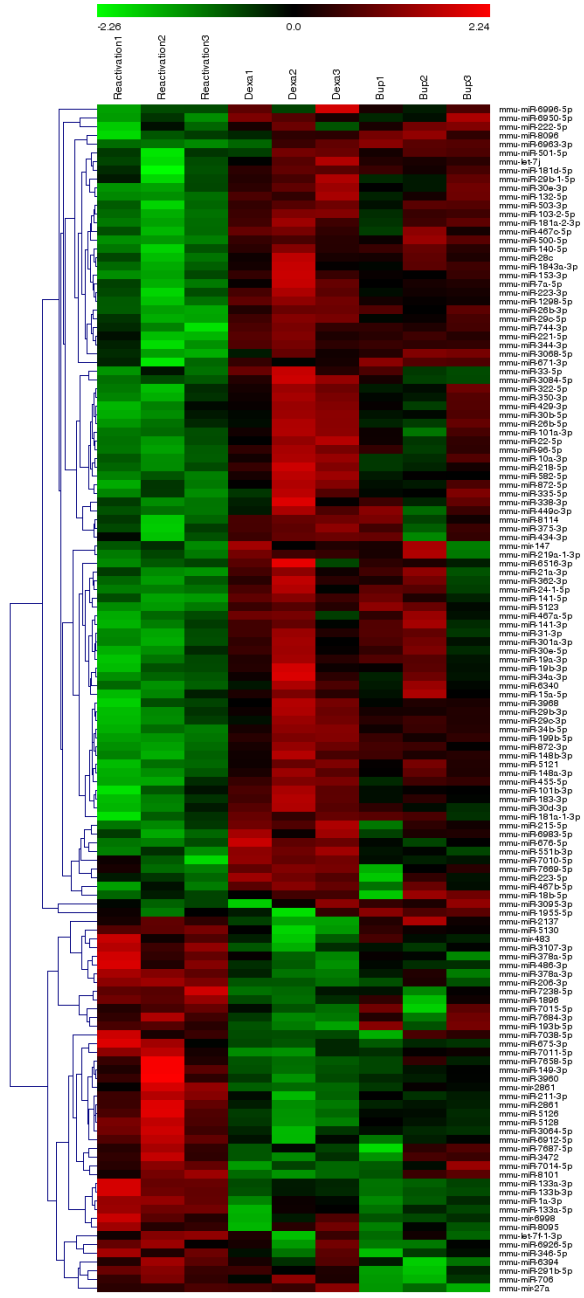

(B)

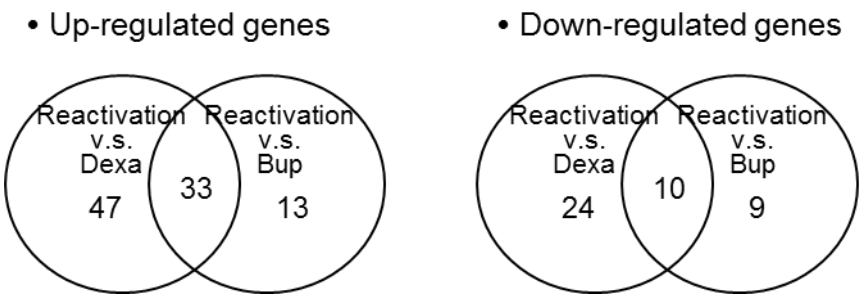

Figure 10. Differentially expressed microRNAs in bupropion, dexamethasone compared to the spontaneous reactivation. Relative expression levels of miRNAs in the heat maps (A) and Venn diagram of the differentially expressed genes in the lung tissues of mice treated with bupropion and dexamethasone (B).

IV. Discussion

The IGRA, which is a more specific and sensitive test than the TST, is currently the most commonly used method to diagnose LTBI, which is based on a cell-mediated immune response. However, both the IGRA and TST have a limitation in that they cannot distinguish between latent and active TB.[17] Accurate latent state detection is important because it represents the starting point of treatment that could reduce the likelihood of reactivation.[18] If patients miss the appropriate treatment period due to an incorrect diagnosis, they can infect many people during those few days.

Recently, IFN-γ, as well as the indicators used in the IGRA and many types of immune-related genes have been proposed as potential biomarkers for identifying the presence or absence of infection with *M. tuberculosis* and the infection stage.[19-21] The selective combination of these genes has been a topic of ongoing study to be able to more accurately distinguish between the latent and active groups.

When studying methods of diagnosis, it is very important to understand the immunopathology of a disease. This is because the expression of immune-related genes differs according to the type and stage of disease.[22] After *M. tuberculosis* enters through the respiratory tract and is phagocytosed by macrophages, the mycobacterial protein and host macrophages interact with each other. The proteins secreted by *M. tuberculosis* interfere with the microbicidal function of the host, and therefore these proteins can be developed into vaccines or diagnostic methods.[23] One way to best understand TB pathogenesis is through analysis of the expression of genes that control this host–pathogen interaction.

Recently, there has been much research to find suitable biomarkers based on analyses of the cytokine/chemokine profile. Cytokines regulate the inflammatory response,[24] and chemokines play an important role in leukocyte recruitment to the site of infection in the early

stage of infection. These actions, including cell growth, differentiation, and activation of leukocytes, result in the stimulation of various effector functions such as chemotaxis, integrin activation, superoxide radical production, and granule enzyme release.[25]

One of the key points to consider in the discovery of an immunological biomarker is how easily the samples can be obtained and whether they can be obtained stably. From this perspective, measurement of cytokine levels of a human body fluid would facilitate a very quick and accurate diagnosis. In most of the studies conducted to date, whole blood collected from the patient is incubated for 16–24 h and then stimulated by treatment with a TB-specific antigen (CFP-10, ESAT-6, and TB7.7). Genetic analysis is then used to detect any genes with increased expression compared to a healthy sample, which would suggest the possibility of a biomarker that can distinguish between healthy and chronic TB. MCP-1 is a major chemokine associated with TB pathogenesis,[26] and plays an important role in the host anti-mycobacterial inflammatory response.[27] In addition, studies have shown that TNF-α or TNF-α receptor-deficient mice are more susceptible to mycobacterial infection.[28] IP-10 interacts with CXCR3, which plays a role in the trafficking of monocytes to activate T-helper cells.[29] MCP-2 functions as a chemotactic factor for many immune cells.[30] Therefore, the use of IP-10 and MCP-2 in combination with IFN-γ has been proposed as a more specific and promising diagnostic biomarker than the IGRA.[31]

However, as mentioned above, this combination cannot overcome the fatal disadvantages of the existing IGRA, and therefore a detection method that can distinguish between healthy, latent, and active TB is still required.

Research to find such a marker is underway using sputum and plasma samples in addition to blood.[32,33] An advantage of the sputum-based test is the ease of obtaining a good-quality sample without requiring surgery from children and extrapulmonary tuberculosis patients with a challenging diagnosis. This is because clinical samples generally must be obtained

from relatively inaccessible sites.[34] In addition, the response to treatment over time can be easily monitored by using a marker found in the saliva.[35]

Recently, it has become common practice to omit the process of stimulation because the diagnosis using *M. tuberculosis* antigen-induced cytokines/chemokines by peripheral blood mononuclear cells is considered to be inconvenient, labor-intensive, and time-consuming.[36] A new approach is to directly measure the levels of cytokines in the plasma.[37] HIV infection does not lead to a difference in the cytokine and chemokine expression levels from plasma without antigen stimulation, although slightly higher gene expression is observed in HIV-positive TB patients.[38] Therefore, this method could yield an efficient diagnosis, maintaining the benefits of the TB-specific existing IGRA while omitting the cumbersome process.

In this study, we aimed to identify biomarkers which can be used for a more sensitive, specific, rapid, and effective diagnosis. In this study, a mouse model was established to reflect the various stages of TB infection, and total RNA was isolated from the lung tissue of mice at the healthy, latent, chronic TB and reactivation stages. Cytokines expression levels were significantly different depending on the stage of infection, which was confirmed by both microarray and RT-qPCR analysis. To find biomarker candidates, several immune-related genes were selected from genes with a large difference between latent and chronic TB.

Several candidate markers appeared to be appropriate for distinguishing between latent and chronic TB infection for selecting candidate markers: *Cxcl9, Cxcl10, Cxcl11, Ccl5, Ccl19, Ccl2 (MCP-1), Ccl7* (MCP-3), *Ccl8* (MCP-2), *Ccl12* (MCP-5), *Tnf, Ifn-γ, Il21r, Il12rβ1, Il12rβ2, Il2rβ, Il7r,* and *Il27rα*.

One consistent finding in TB patients is that the expression of IFN-γ, TNF-α, CXCL9, CXCL10, and CXCL11 tends to be higher in active TB than healthy.[39] Specially, IFN-γ and CXCL10 are already well-known major biomarkers for TB. Our results are in agreement with

those of previous studies, and are not surprising given that CXCL10 is known to be under the regulation of IFN-γ. However, our study also showed that the expression of CXCL10 was much higher than that of IFN-γ; therefore, CXCL10 may be easier to detect. Furthermore, because the changes in CXCL10 levels were more significant than those in IFN-γ levels, CXCL10 could be a more useful biomarker to screen the infection stages of TB. In addition to IFN-γ and CXCL10, our study suggested that chemokines such as CXCL9, CXCL11, CCL7, and CCL12 were increased distinctly in the chronic stage relative to the latent stage. Similar to our results, the plasma levels of CXCL9, CXCL10, and CXCL11 were reported in another study to be higher in active TB patients than in healthy persons, whereas the IFN-γ levels did not differ in that paper. A recent study also showed that levels of CXCR3 ligands, such as CXCL9 and CXCL11, were higher in sera from TB patients than in sera from healthy persons. However, there has been no report about CCL7 and CCL12 until this present work. In our study, the significant differences between the chronic stage and the latent or healthy stages suggest these ligands as biomarker candidates. To more accurately distinguish between these stages, the selective combination of immune response genes should be under study.

This match in the variation of TB-specific immune genes with those identified in the present study provides a basis to support a common TB pathogenesis between humans and mice. This similarity may help to improve the understanding of complex infectious diseases and the mechanism of the human immune response using animal models without the need for surgical procedures.[40] In particular, a cross-over study of experimental models can be used for diagnosis and treatment monitoring, and may also be actively used in research and vaccine development.

In order to identify biomarkers that can distinguish the stage of TB infection using miRNA, we experimented with the same scheme. Research on miRNAs has not been around for a long time, and efforts to use them as biomarkers have not been in less than 10 years, so many of

its functions and targets have not yet been identified. In our study, it is clear that mmu-miR-206-3p is the best marker to distinguish between latent and spontaneous reactivation and mmu-miR-1a-3p is an exceptional marker that can distinguish healthy, latent, chronic TB and spontaneous reactivation at the same time. If their functions and targets are studied, they will help to understand the pathology that changes when infected with TB and will be supported by evidence as a diagnostic marker for tuberculosis.

In conclusion, we have identified several new biomarkers that may be applied for TB screening and for the diagnosis of active TB/reactivation. Of particular importance, we suggest evidence that the combined use of multiple indicators may raise the sensitivity and specificity of TB detection. If the proposed biomarkers CXCL9, CCL7, CCL12, mmu-miR-1a-3p and mmu-miR-206-3p show the same tendency in human lesions as in mice, they could be combined and used as highly promising diagnostic markers.

References

1. Zumla A, Raviglione M, Hafner R, von Reyn CF. Tuberculosis. N Engl J Med 2013;368:745-55.
2. Dye C, Williams BG. The population dynamics and control of tuberculosis. Science 2010;328:856-61.
3. Lawn SD, Zumla AI. Tuberculosis. Lancet 2011;378:57-72.
4. Lee SW, Wu LS, Huang GM, Huang KY, Lee TY, Weng JT. Gene expression profiling identifies candidate biomarkers for active and latent tuberculosis. BMC Bioinformatics 2016;17 Suppl 1:3.
5. Comstock GW, Livesay VT, Woolpert SF. The prognosis of a positive tuberculin reaction in childhood and adolescence. Am J Epidemiol 1974;99:131-8.
6. Herrera V, Perry S, Parsonnet J, Banaei N. Clinical application and limitations of interferon-gamma release assays for the diagnosis of latent tuberculosis infection. Clin Infect Dis 2011;52:1031-7.
7. Mandalakas AM, Hesseling AC, Chegou NN, Kirchner HL, Zhu X, Marais BJ, et al. High level of discordant IGRA results in HIV-infected adults and children. Int J Tuberc Lung Dis 2008;12:417-23.
8. Jacobsen M, Repsilber D, Gutschmidt A, Neher A, Feldmann K, Mollenkopf HJ, et al. Candidate biomarkers for discrimination between infection and disease caused by Mycobacterium tuberculosis. J Mol Med (Berl) 2007;85:613-21.
9. Walter ND, Miller MA, Vasquez J, Weiner M, Chapman A, Engle M, et al. Blood Transcriptional Biomarkers for Active Tuberculosis among Patients in the United States: a Case-Control Study with Systematic Cross-Classifier Evaluation. J Clin Microbiol 2016;54:274-82.
10. Jayakumar A, Vittinghoff E, Segal MR, MacKenzie WR, Johnson JL, Gitta P, et al.

Serum biomarkers of treatment response within a randomized clinical trial for pulmonary tuberculosis. Tuberculosis (Edinb) 2015;95:415-20.

11. Weiner J, 3rd, Kaufmann SH. Recent advances towards tuberculosis control: vaccines and biomarkers. J Intern Med 2014;275:467-80.
12. He L, Hannon GJ. MicroRNAs: small RNAs with a big role in gene regulation. Nat Rev Genet 2004;5:522-31.
13. Huang Y, Shen XJ, Zou Q, Wang SP, Tang SM, Zhang GZ. Biological functions of microRNAs: a review. J Physiol Biochem 2011;67:129-39.
14. Ambros V. The functions of animal microRNAs. Nature 2004;431:350-5.
15. Zhou MY, Yu GY, Yang XT, Zhu CM, Zhang ZZ, Zhan X. Circulating microRNAs as biomarkers for the early diagnosis of childhood tuberculosis infection. Molecular Medicine Reports 2016;13:4620-6.
16. Wang C, Yang S, Sun G, Tang X, Lu S, Neyrolles O, et al. Comparative miRNA expression profiles in individuals with latent and active tuberculosis. PLoS One 2011;6:e25832.
17. Metcalfe JZ, Everett CK, Steingart KR, Cattamanchi A, Huang L, Hopewell PC, et al. Interferon-gamma release assays for active pulmonary tuberculosis diagnosis in adults in low- and middle-income countries: systematic review and meta-analysis. J Infect Dis 2011;204 Suppl 4:S1120-9.
18. Parida SK, Kaufmann SH. The quest for biomarkers in tuberculosis. Drug Discov Today 2010;15:148-57.
19. Ruhwald M, Bjerregaard-Andersen M, Rabna P, Eugen-Olsen J, Ravn P. IP-10, MCP-1, MCP-2, MCP-3, and IL-1RA hold promise as biomarkers for infection with M. tuberculosis in a whole blood based T-cell assay. BMC Res Notes 2009;2:19.
20. Liang Y, Wang Y, Li H, Yang Y, Liu J, Yu T, et al. Evaluation of a whole-blood chemiluminescent immunoassay of IFN-gamma, IP-10, and MCP-1 for diagnosis of

active pulmonary tuberculosis and tuberculous pleurisy patients. APMIS 2016.

21. Suzukawa M, Akashi S, Nagai H, Nagase H, Nakamura H, Matsui H, et al. Combined Analysis of IFN-gamma, IL-2, IL-5, IL-10, IL-1RA and MCP-1 in QFT Supernatant Is Useful for Distinguishing Active Tuberculosis from Latent Infection. Plos One 2016;11.

22. Djoba Siawaya JF, Chegou NN, van den Heuvel MM, Diacon AH, Beyers N, van Helden P, et al. Differential cytokine/chemokines and KL-6 profiles in patients with different forms of tuberculosis. Cytokine 2009;47:132-6.

23. Kim K, Sohn H, Kim JS, Choi HG, Byun EH, Lee KI, et al. Mycobacterium tuberculosis Rv0652 stimulates production of tumour necrosis factor and monocytes chemoattractant protein-1 in macrophages through the Toll-like receptor 4 pathway. Immunology 2012;136:231-40.

24. Slight SR, Khader SA. Chemokines shape the immune responses to tuberculosis. Cytokine Growth Factor Rev 2013;24:105-13.

25. Gale LM, McColl SR. Chemokines: extracellular messengers for all occasions? Bioessays 1999;21:17-28.

26. Ma J, Jung BG, Yi N, Samten B. Early Secreted Antigenic Target of 6 kDa of Mycobacterium tuberculosis Stimulates Macrophage Chemoattractant Protein-1 Production by Macrophages and Its Regulation by p38 Mitogen-Activated Protein Kinases and Interleukin-4. Scand J Immunol 2016;84:39-48.

27. Roach DR, Bean AG, Demangel C, France MP, Briscoe H, Britton WJ. TNF regulates chemokine induction essential for cell recruitment, granuloma formation, and clearance of mycobacterial infection. J Immunol 2002;168:4620-7.

28. Bean AG, Roach DR, Briscoe H, France MP, Korner H, Sedgwick JD, et al. Structural deficiencies in granuloma formation in TNF gene-targeted mice underlie the heightened susceptibility to aerosol Mycobacterium tuberculosis infection, which is

not compensated for by lymphotoxin. J Immunol 1999;162:3504-11.

29. Farber JM. Mig and IP-10: CXC chemokines that target lymphocytes. J Leukoc Biol 1997;61:246-57.

30. Moser B, Loetscher P. Lymphocyte traffic control by chemokines. Nat Immunol 2001;2:123-8.

31. Ruhwald M, Bodmer T, Maier C, Jepsen M, Haaland MB, Eugen-Olsen J, et al. Evaluating the potential of IP-10 and MCP-2 as biomarkers for the diagnosis of tuberculosis. Eur Respir J 2008;32:1607-15.

32. Marais BJ, Pai M. New approaches and emerging technologies in the diagnosis of childhood tuberculosis. Paediatr Respir Rev 2007;8:124-33.

33. Sia IG, Wieland ML. Current concepts in the management of tuberculosis. Mayo Clin Proc 2011;86:348-61.

34. Lee JY. Diagnosis and treatment of extrapulmonary tuberculosis. Tuberc Respir Dis (Seoul) 2015;78:47-55.

35. Jacobs R, Tshehla E, Malherbe S, Kriel M, Loxton AG, Stanley K, et al. Host biomarkers detected in saliva show promise as markers for the diagnosis of pulmonary tuberculosis disease and monitoring of the response to tuberculosis treatment. Cytokine 2016;81:50-6.

36. Yang QT, Cai Y, Zhao W, Wu F, Zhang MX, Luo K, et al. IP-10 and MIG Are Compartmentalized at the Site of Disease during Pleural and Meningeal Tuberculosis and Are Decreased after Antituberculosis Treatment. Clinical and Vaccine Immunology 2014;21:1635-44.

37. Xiong WJ, Dong HP, Wang JJ, Zou XM, Wen Q, Luo W, et al. Analysis of Plasma Cytokine and Chemokine Profiles in Patients with and without Tuberculosis by Liquid Array-Based Multiplexed Immunoassays. Plos One 2016;11.

38. Mihret A, Bekele Y, Bobosha K, Kidd M, Aseffa A, Howe R, et al. Plasma cytokines

and chemokines differentiate between active disease and non-active tuberculosis infection. Journal of Infection 2013;66:357-65.

39. Kim S, Lee H, Kim H, Kim Y, Cho JE, Jin H, et al. Diagnostic performance of a cytokine and IFN-gamma-induced chemokine mRNA assay after Mycobacterium tuberculosis-specific antigen stimulation in whole blood from infected individuals. J Mol Diagn 2015;17:90-9.

40. O'Garra A. Systems approach to understand the immune response in tuberculosis: an iterative process between mouse models and human disease. Cold Spring Harb Symp Quant Biol 2013;78:173-7.

Abstract (in Korean)

마우스에서 결핵균 감염 상태에 따른 유전자 발현의 차이

<지도교수 최인홍>

연세대학교 대학원 의과학과

박수민

결핵의 원인은 대부분 *Mycobacterium tuberculosis* 이며, 감염성 질병 중에서 사망률이 세계 2위에 랭크되어 있는 심각한 질병이다. WHO는 2013년까지 *M. tuberculosis* 에 감염되어 발병된 사람은 900만 명, 사망자는 150만 명이라고 밝혔다. 현재 전체 인구의 약 1/3, 즉 20억 명 이상이 TB 잠복 감염자인 것이다. 그 중 5-10% 만이 활동성 결핵 환자가 되는데, 대부분 면역력이 약화된 사람이나 AIDS 환자, 흡연자 또는 당뇨병 환자이다. 잠복감염자에게는 증상이 나타나지도 않고 감염성도 없지만, 결핵환자가 될 수 있는 가능성을 갖고 있으므로 정확한 진단을 통해 잠복감염 상태인지 확인하는 것이 결핵을 퇴치할 수 있는 가장 효율적인 방법이다. 따라서 현존하는 결핵 진단법보다 더 효율적이고 특이적인 바이오 마커의 발굴이 필요하다.

결핵균을 공기 감염시켜 만든 C57BL/6 마우스 모델을 이용하여 잠복결핵, 활동성 결핵, 재활성화, 그리고 면역억제제를 처리한 그룹을 만들었다. 각 감염

단계에 따라 다르게 발현하는 면역 관련 유전자와 microRNA를 이용하여 결핵 진단을 판단할 수 있는 지표를 설정하고자 실험하였다.

먼저, 건강한 마우스, 잠복결핵, 활동성 결핵 마우스의 폐 조직에서 RNA를 분리한 다음, microarray 분석을 수행하였고, 이 결과를 확인하기 위해 real-time PCR 하였다. 잠복결핵과 활동성 결핵을 구분하기 위한 목적에 부합하는 17개의 바이오 마커 후보물질을 골랐고 4가지 그룹으로 분류하였다: 1) monocyte chemoattractant proteins (MCPs)를 제외한 chemokines (CXCL9, CXCL10, CXCL11, CCL5, CCL19); 2) MCPs (CCL2, CCL7, CCL8, CCL12); 3) Receptors (IL2Rβ, IL7R, IL12Rβ1, IL12Rβ2, IL21R, IL27Rα); 4) TNF, IFN-γ. 이 유전자들은 잠복결핵에 비해 활동성 결핵 마우스에서 높은 발현을 보였으며($p < 0.05$), 특히 CXCL9, CCL7, CCL12 가 가장 특이적이고 정확한 마커로써 기능을 할 것이라 판단한다. 마우스 조직뿐 아니라, 혈청에서도 같은 경향성을 나타내는지 확인하기 위해 luminex assays를 이용하여 단백질 발현 정도를 확인하였다. 건강한 마우스의 혈청에서 CCL7과 CCL12의 발현 차이가 커서 유의한 결과를 얻을 수는 없었지만, 잠복결핵에 비해 활동성 결핵에서 더 높은 발현을 나타냄을 확인하였다.

이번에는 건강한 마우스, 잠복결핵, 활동성 결핵뿐만 아니라, 재활성화된 마우스 (자발적 재활성화, 면역억제제-bupropion, dexamethasone를 처리한 마우스)를 설정하여 각 단계의 폐 조직에서 miRNA를 분리하였다. 마찬가지로 microarray와 real-time PCR을 수행한 뒤, 각 감염상태를 구분할 수 있는 10가지의 microRNA를 골랐다: mmu-miR-1a-3p, mmu-miR-133a-5p, mmu-miR-133a-3p, mmu-miR-206-3p, mmu-miR-133b-3p, mmu-miR-3064-5p, mmu-miR-450b-3p, mmu-miR-26b-3p, mmu-miR-181a-2-3p, mmu-miR-8114. 그 중에서 특히 miR-206-3p가

잠복결핵이나 활동성 결핵에 비해 재활성화된 마우스에서 발현이 크게 증가하는 것을 확인할 수 있었다($p < 0.05$). 또한 mmu-miR-1a-3p의 발현 차이로 잠복결핵, 활동성 결핵 그리고 자발적 재활성화가 일어난 마우스를 동시에 구분할 수 있으며, 이것이 바이오 마커의 가장 적절한 후보물질이 될 수 있다.

실험을 통해 결핵 감염 상태에 따른 유전자 발현의 차이를 명확하게 확인할 수 있었고, 이러한 차이가 결핵균에 대한 숙주의 방어기작에 중요한 역할을 할 것이라 여겨진다. 기존의 논문에 제시되지 않은 몇 가지 바이오 마커의 물질을 제시했다는 데 의의가 있으며, cytokine과 miRNA를 혼합하여 마커로 이용한다면 현존하는 진단법보다 훨씬 정확하고 특이성 높은 진단법을 구축할 수 있을 것이라 판단한다.

핵심되는 말: Tuberculosis, Cytokine, Chemokine, MicroRNA, Latent, Chronic, Reactivation, Bupropion, Dexamethasone